Specifications for Tools Used in Structural Field Testing of Flexible Pavement Layers

Research Project 0-1735
Development of Structural Field Testing of
Flexible Pavement Layers

Conducted for
Texas Department of Transportation
in cooperation with
Federal Highway Administration

Technical Memorandum 1735-1
March 1997

Center for Highway Materials Research
The University of Texas at El Paso
El Paso, TX 79968
(915) 747-6925

Executive Summary

This report contains the specifications for the equipment to be developed, and demonstration of methodology to be used to determine engineering properties of flexible pavements during construction. The primary goal of this project is to develop realistic field protocols and test equipment, which in a rational manner, combine the results from laboratory and field tests with those used for quality control during construction. The significance of the project is that more rational methods for quality control during construction can be developed, at the same time, feedback to the pavement design engineer can be provided in terms of the asumption made to design the pavement.

Depending upon the thickness of different layers and mode of failure different parameters pay dominant roles. But in general the most important parameters are the thickness and moduli of different layers as well as Poisson's ratio of subgrade. These parameters should be measured fairly accurately. Tests to measure most of these parameters are included in the specifications presented herein.

The concentration of the project will be towards developing three devices, in addition to evaluating the FWD and GPR. These devices are:

■ The portable Seismic Pavement Analyzer originally developed for rapid evaluation of surface layer will be modified so that it can be used on top of the base and/or the prepared subgrade.

■ A dynamic cone penetration device will be retrofitted with appropriate sensors, so that the elastic modulus and Poisson's ratio of the subgrade can be determined rapidly and with minimal disturbance.

■ A combined deflection/seismic device will be designed. In such a device, the diagnostic powers of seismic methods can be simultaneously utilized in conjunction with the advantages of the FWD as a design tool.

The main concentration of the study is towards seismic methods because hey measure a fundamentally correct property of the material (i.e. elastic modulus), and in the most part, they can be duplicated in the laboratory. No other existing method has this capability.

The technical aspects of each test method suggested above, along with institutional and nontechnical parameters to be considered, are important. Most tests are relatively rapid to perform, and depending on the level of sophistication devices will cost between $10,000 to

$100,000. They all require short period of training for performing the tests with these devices, and a longer term training for interpreting the results.

Several case studies are included to show the level of sophistication in data collection, typical outcome from tests, and correlation with conventional methods. The following lessons learned from these case studies which should be thoroughly studied in the remainder of this project:

■ Laboratory tests show that seismic tests are rather repeatable with a repeatability of better than 90 percent.

■ In the field, the seismic modulus is sensitive to small variations in moisture content and dry density of the base and prepared subgrade.

■ The CBR value of the base determined from DCP tests generally increase as the seismic modulus increases.

■ For granular materials, moduli from laboratory seismic tests are in good agreement with seismic field moduli as long as the laboratory specimens are prepared at the density and moisture content of the field materials. If the specimens are prepared as per Tex-111-E, the laboratory moduli are significantly smaller.

■ For granular materials, the laboratory resilient moduli are typically much less than the seismic moduli; this can be attributed to the boundary conditions and the method of sample preparation associated with resilient modulus tests.

■ For granular materials, seismic moduli and FWD moduli show similar trends; that is both generally increase; however, they are not related by a unique relationship.

■ For AC layer, the seismic moduli measured in situ and seismic moduli measured in the laboratory are quite close.

In the continuation of this project, several issues should be addressed. These issues consists of the following items:

■ Develop more comprehensive relationships between the moisture content and dry unit weight and modulus of granular materials.

■ Develop relationships between the volumetric properties of ACP and the modulus through monitoring the moduli of specimens prepared for mix design.

- Optimize the source-receiver configuration as a function of the thickness of layers for the PSPA.

- Optimize the source for the granular materials so that enough energy can be coupled into the medium.

- Optimize the coupling of the seismic DCP to the base and subgrade.

- Develop a simplified algorithm for real-time reduction of the DCP data.

- Optimize the source-receiver configuration for the combined seismic/deflection device

- Develop an adequate calibration process for the combined seismic/deflection device

Table of Content

List of Tables

List of Figures

Specifications for Tools Used in Structural Field Testing of Flexible Pavement Layers

1. Introduction

Aside from traffic and environmental loading, the primary parameters that affect the performance of a flexible pavement section are the modulus, thickness, and Poisson's ratio of each layer. Current TxDOT procedure for structural design of flexible pavements considers these parameters. The Materials and Tests Division has acquired the state-of-the-art equipment and training to perform laboratory resilient modulus tests on AC, base and subgrade materials. The Design Division can perform nondestructive field tests to estimate the in-place moduli of different layers. Unfortunately, the construction specifications are not based on these engineering properties. The acceptance criteria are typically based on adequate thickness, and adequate density of the placed and compacted materials. To successfully implement any mechanistic pavement design procedure, and to move towards performance-based specifications, it is essential to develop tools that can measure the modulus, thickness and Poisson's ratio of each layer. The main objective of this project is to develop inexpensive and precise devices for project level studies.

The primary goal of this project is to develop realistic field protocols and test equipment, which in a rational manner, combine the results from laboratory and field tests with those used for quality control during construction. A series of simplified laboratory tests that are compatible with the field tests will be used. All these tests have several features in common. They can be perform rapidly (less than five minutes), they are inexpensive, and their data reduction processes are simple and almost instantaneous. These technologies can be transferred to TxDOT.

The significance of this project is evident. These types of tests are one of the major components needed to develop a mechanistic pavement design and a performance-based construction specification. A gradual transition from the existing specifications to performance-based specifications may be necessary. Performing the simplified laboratory and field tests on pavement materials will allow us to develop a database that can be used to smoothly unify the design procedures and construction quality control.

In this report, field procedures to measure the modulus, Poisson's ratio, and thickness of each pavement layer shortly after placement and after the completion of the project are presented.

Specifically, we will be concentrating on three devices:

- The portable Seismic Pavement Analyzer originally developed for rapid evaluation of surface layer will be modified so that it can be used on top of the base and/or the prepared subgrade.

- A dynamic cone penetration device will be retrofitted with appropriate sensors, so that the elastic modulus and Poisson's ratio of the subgrade can be determined rapidly and with minimal disturbance.

- A combined deflection/seismic device will be designed. In such a device, the diagnostic powers of seismic methods can be simultaneously utilized in conjunction with the advantages of the FWD as a design tool.

The main pavement parameters that are important to a mechanistic pavement design should be established. The significance of each parameter is qualified through a sensitivity study in section 2.

All these tools have one thing in common — they measure seismic wave velocities. Seismic wave velocities can be readily transformed to moduli using fundamentally correct relationships. Moduli of different layers are one of the main parameters input in any mechanistic pavement design for flexible pavements. A discussion on the nature of the moduli measured with the seismic methods is included in section 3.

A brief description of each method is included in section 4. A short background on the wave propagation theory is included in Appendix A, where the relationships between wave velocity and modulus are established. The cost and operational parameters of each device are also described in section 4.

To be effective in practical use, a device should have four major features. First, it should measure fundamental properties of materials (i.e., it should not be an index test). Second, the device should be _sensitive enough_ to the parameter of interest so that good and bad quality materials can be readily delineated. Third, the measurements should be _accurate enough_ so that they can provide feedback to the designer and the laboratory personnel. Fourth, the device should be _precise enough_ so that it can be readily used in the QA/QC process. These levels are also defined in sections 2 and 4.

Several case studies are included in section 5 to show some results that can possibly be obtained with some of the devices.

The last section itemizes the technical problems that should be solved in the next 2.5 years in this project.

2. Determination of Significant Design Parameters

Fatigue and rutting are the two major factors that contribute to the structural loss of life in a pavement. The number of repeated ESALs, which causes the fatigue cracking damage to the pavement is a function of the tensile strain at the bottom of the asphaltic layer, ε_t, and the modulus of the asphalt layer, E_R. The most common relationship for the remaining life of a pavement due to fatigue cracking, N_F, is (Finn et al. 1977):

$$\log N_F = 15.947 - 3.291 \log\left(\frac{\varepsilon_t}{10^{-6}}\right) - 0.854 \log\left(\frac{E_R}{10^3}\right) \tag{2-1}$$

The number of ESALs which cause the rutting failure, N_R, is a function of the compressive strain at the top of the subgrade, ε_{vs}. For computing the remaining life due to rutting, the equation developed by Shook et al. (1982) is commonly used. This relationship is:

$$N_R = 1.077 \times 10^{18} \left(\frac{10^{-6}}{\varepsilon_{vs}}\right)^{4.4843} \tag{2-2}$$

A stochastic sensitivity analysis was conducted to assess the influence of layer thickness, layer moduli and Poisson's ratio on the predicted remaining life of a pavement system.

The methodology used to carry out the study can be summarized in the following steps:

1. The pavement parameters (modulus, thickness and Poisson's ratio) were taken as random variables one at a time for the following four different pavement sections:

    - thin AC (75 mm), thin base (150 mm),
    - thin AC (75 mm), thick base (300 mm),
    - thick AC (125 mm), thin base (150 mm),
    - thick AC (125 mm), thick base (300 mm).

    The other parameters of the pavement profiles were assumed to be constant as shown in Table 2.1.

2. Assigning a coefficient variation of 10 percent, 100 sample values for each pavement parameter were generated using Monte Carlo simulation techniques.

3. For each simulated sample set, the remaining lives due to fatigue cracking and rutting were calculated, and compared to the remaining lives from the values in Table 2.1. The variation from the baseline design was calculated from:

$$Variation\ (percent) = \frac{RL_{purturbed} - RL_{baseline}}{RL_{baseline}} 100\% \qquad (2.3)$$

where $RL_{purturbed}$ and $RL_{baseline}$ correspond to the remaining lives from the baseline pavement profile and the perturbed pavement profile, respectively.

4. Based on the variations of the remaining lives from the baseline, the factors that significantly affect the remaining life were identified. A set of arbitrary limits were used to define the significance of a given parameter in the remaining life. These levels are defined in Table 2.2.

Table 2.1 - Properties of Typical Pavement Sections Selected for This Study

Parameter	Layer	Value
Thickness	AC (t_1)	75 mm or 150 mm
	Base (t_2)	150 mm or 300 mm
Modulus	AC (E_1)	3.5 GPa
	Base (E_2)	350 MPa
	Subgrade (E_3)	70 MPa
Poisson's Ratio	AC (v_1)	0.35
	Base (v_2)	0.40
	Subgrade (v_3)	0.45

Typical comparisons of the remaining lives with respect to the baseline design due to fatigue and rutting for a pavement with thin AC and thin base layers are shown in Figure 2.1. The baseline remaining lives refer to the remaining lives calculated from the parameters indicated in Table 2.1 before any perturbation of a parameter. To determine if a parameter is sensitive to a certain model, the standard deviation of the remaining life associated with that parameter is compared with the 10 percent perturbation allowed. Depending on whether the standard deviation is larger or smaller than 10 percent input, one can judge if the parameter is sensitive or not sensitive to a certain design.
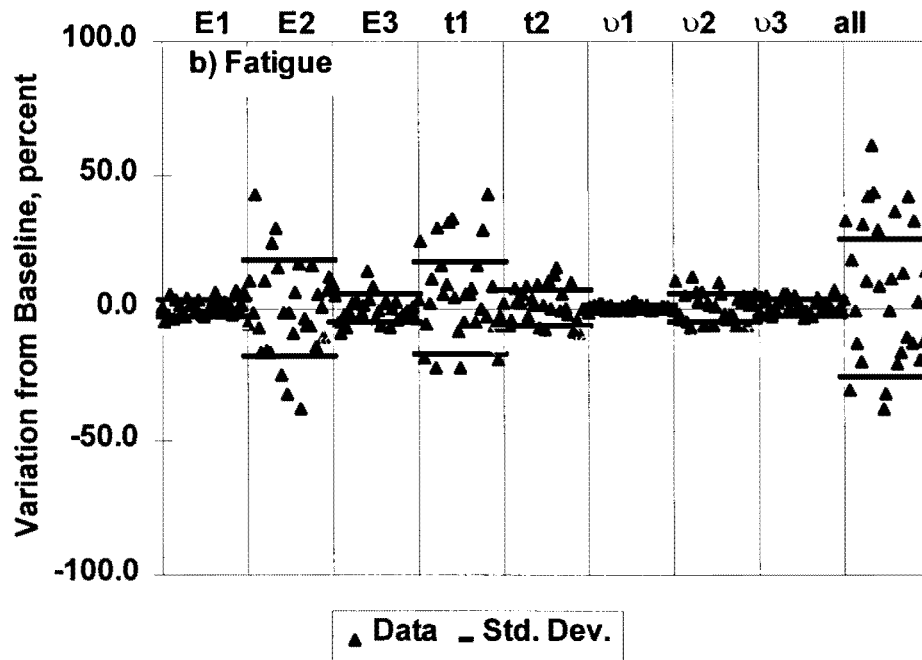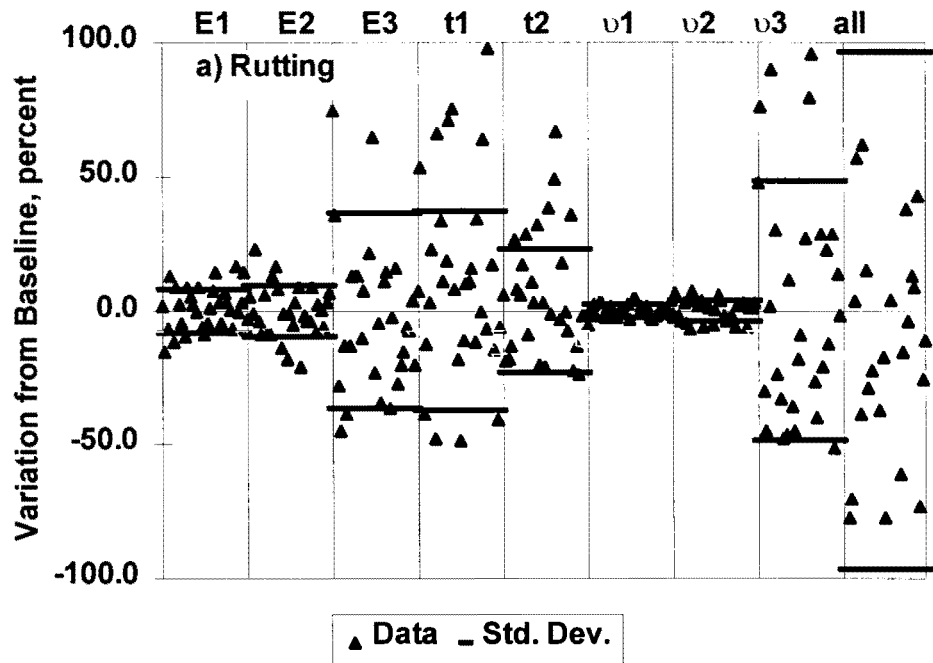
Figure 2.1 - Sensitivity of Different Pavement Parameters on Remaining Life of a
Typical Pavement with Thin AC and Thin Base

From Figure 2.1a, a 10 percent variation in Poisson's ratios of the AC (v_1) and base (v_2) results in a very small variation in the remaining life due to rutting. Therefore, these two parameters are categorized as insignificant. On the other hand, varying the modulus of subgrade (E_3) or the thickness of AC (t_1) or the Poisson's ratio of subgrade (v_3) by 10 percent would change the remaining life due to rutting by more than 25 percent. Therefore, these three parameters are considered as very significant.

Table 2.2 - Level of Significance Assigned to each Parameter Based on a 10% Perturbation of Original Input Parameter

Level of Significance	Criteria in Terms of Coefficient of Variation	Symbol	Significance to This Study
Insignificant	< 5 percent	I	Can be probably estimated with small error in final remaining life
Moderately Significant	5-15 percent	M	Must be measured to limit errors in design
Significant	15-25 percent	S	Must be measured reasonably accurately for satisfactory design
Very Significant	> 25 percent	V	Must be measured very accurately or design may not be considered appropriate

The results from the four sections studied are shown in Figures 2.2 through 2.4, and are summarized in Table 2.3. Depending on the thickness of pavement layers, different parameters are of different significance; that is, one parameter that maybe significant in one case may be of less significance in a thicker or thinner pavement.

Based on this study, the parameters itemized in Table 2.4 significantly affect the remaining life of a flexible pavement. Therefore, not only the modulus of each layer should be accurately measured, the thickness and Poisson's ratio of some layers should also be known.

The modulus and Poisson's ratio can be determined either with field testing or with laboratory testing. For a more sophisticated analysis, the behavior of the material in terms of variation in stiffness with stress level, strain amplitude, and the strain rate should be determined. This behavior is typically established by conducting laboratory tests such as the resilient modulus test. These tests are time-consuming. Practically speaking, only one or two specimens can be tested for each project. Simplified laboratory tests can be used in

Table 2.3 - Significance of Pavement Parameters in Remaining Life of Pavement

Parameter	Layer	Relative Significance							
		Rutting				Fatigue			
		Thin AC		Thick AC		Thin AC		Thick AC	
		Thin Base	Thick Base	Thin Base	Thick Base	Thin Base	Thick Base	Thin Base	Thick Base
Thickness	AC (t_1)	V	V	V	V	M	I	M	I
	Base (t_2)	V	S	V	V	M	S	V	V
Modulus	AC (E_1)	M	M	M	M	I	I	M	M
	Base (E_2)	M	M	I	M	M	S	S	S
	Subgrade (E_3)	S	V	M	V	M	M	M	M
Poisson's Ratio	AC (v_1)	I	I	I	I	I	I	I	I
	Base (v_2)	I	M	I	M	M	M	I	M
	Subgrade (v_3)	V	V	V	V	I	I	I	I

Table 2.4 - Parameters that Affect Remaining Life of Flexible Pavements

Failure Criteria	Important Pavement Parameters[*]
Fatigue Cracking	• Thickness of Base • Modulus of Base • Modulus of Subgrade • Poisson's Ratio of Base • Modulus of AC • Thickness of AC
Rutting	• Thickness of AC • Poisson's Ratio of Subgrade • Thickness of Base • Modulus of Subgrade • Modulus of AC • Modulus of Base

[*] Parameters are sorted with regards to their order of significance
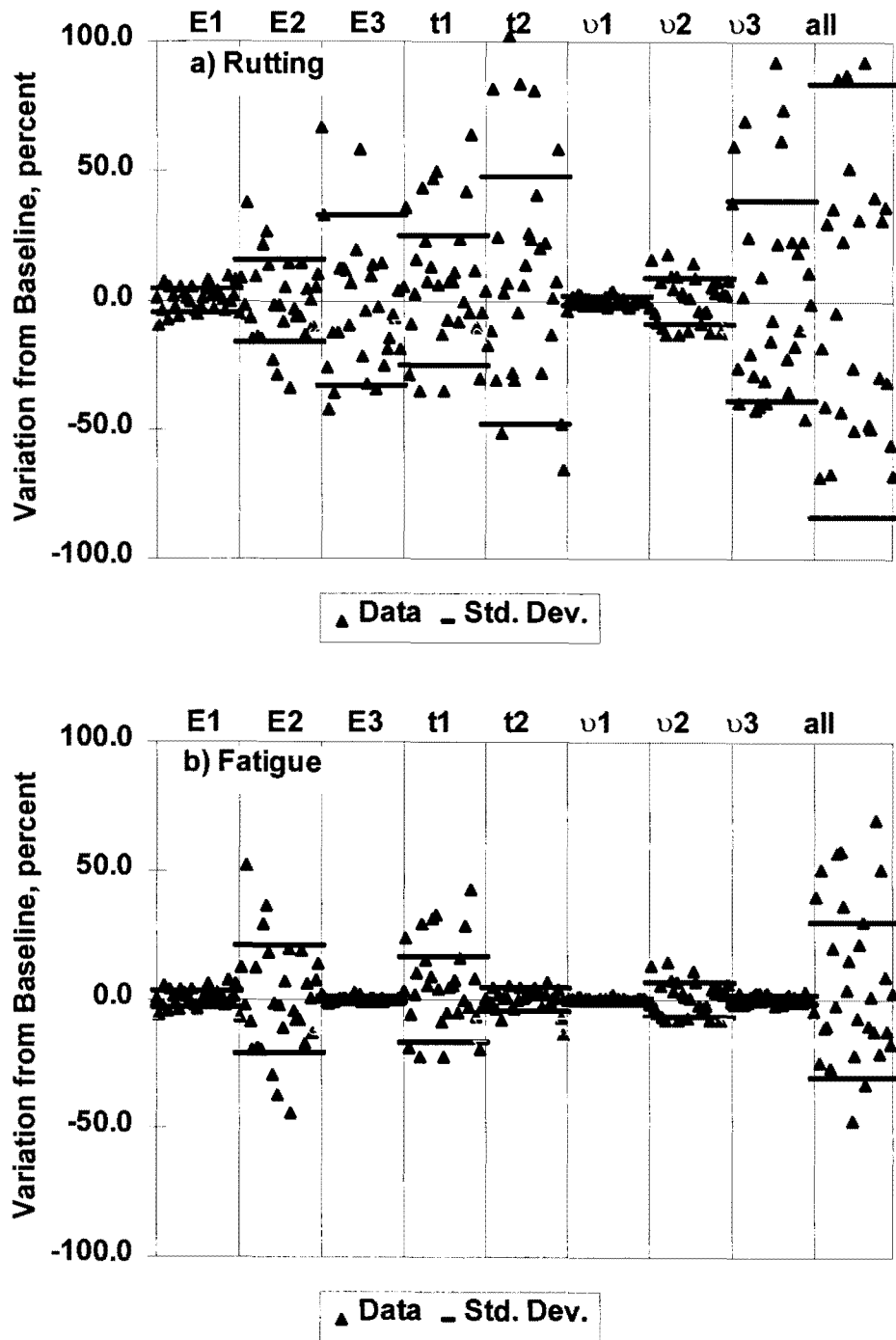
Figure 2.2 - Sensitivity of Different Pavement Parameters on Remaining Life of a Typical Pavement with Thin AC and Thick Base
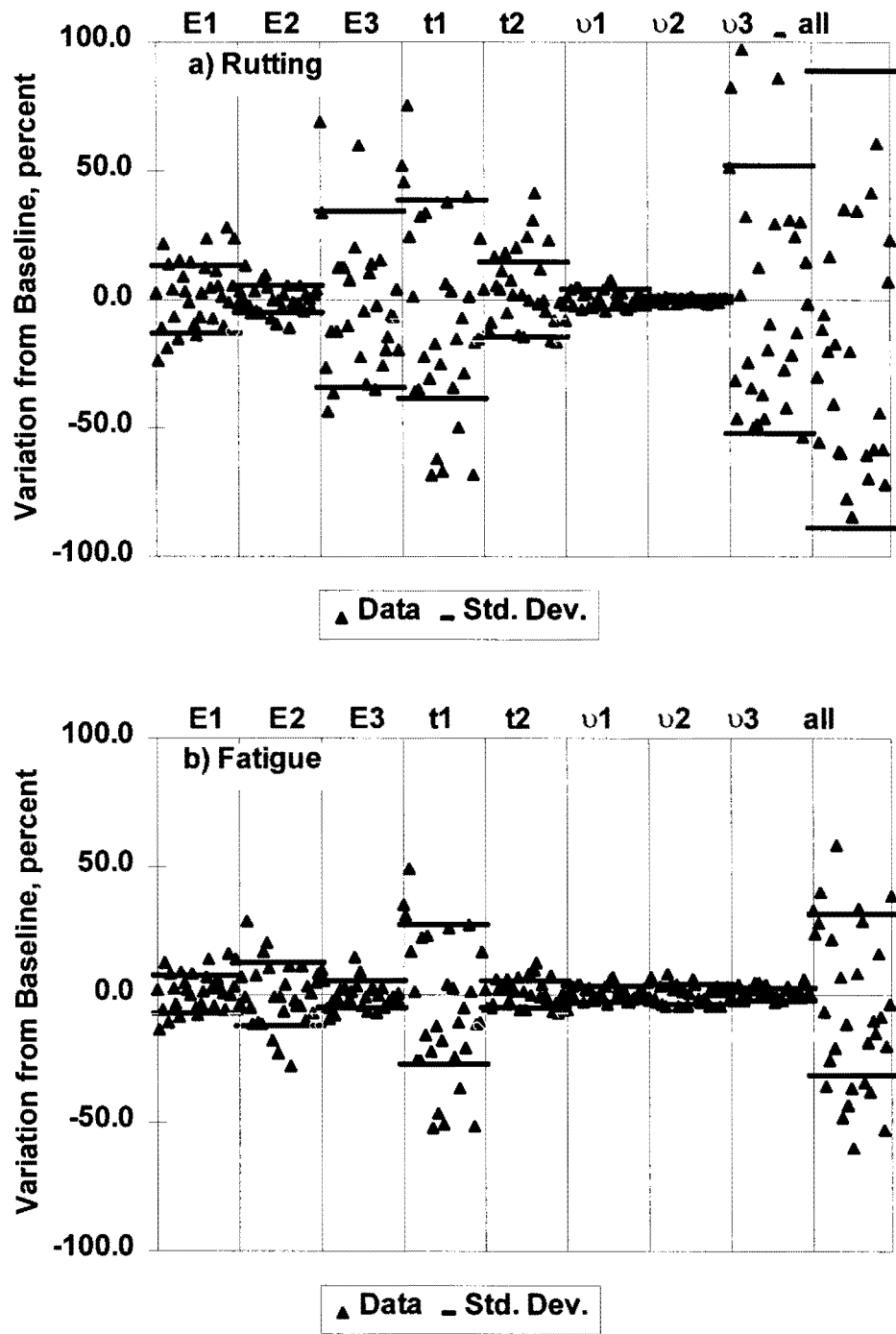
Figure 2.3 - Sensitivity of Different Pavement Parameters on Remaining Life of a Typical Pavement with Thick AC and Thin Base
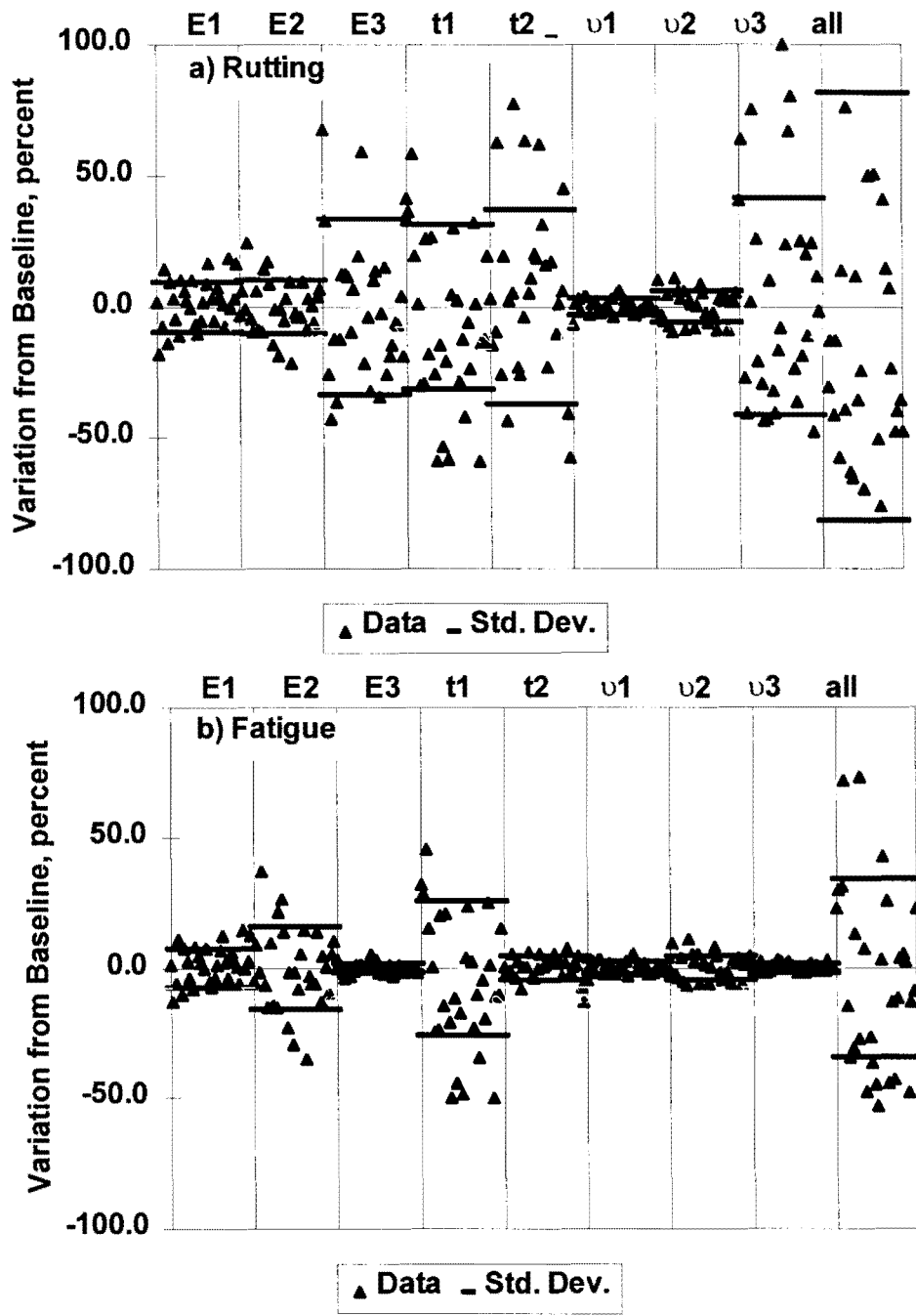
Figure 2.4 - Sensitivity of Different Pavement Parameters on Remaining Life of a Typical Pavement with Thick AC and Thick Base

conjunction with the more sophisticated ones during the design process. By combining the results from simplified and more comprehensive tests, one can either ensure compatibility or can develop correlations that can readily be used in the field.

One significant point to consider has to do with the differences and similarities between material characterization and design simulation. In material characterization one attempts, in a way that is the most theoretically-correct, to determine the engineering properties of a material (such as modulus or strength). The material properties measured in this way, are fundamental material properties that are not related to a specific modelling scenario. To use these material properties in a certain design methodology, they should be combined with an appropriate analytical or numerical model to obtain the design output. In the design simulation, one tries to her/his best ability to experimentally simulate the design condition, and then back-figure some material parameter that is relevant only to that condition. The seismic methods can be considered as methods that provide material characterization; whereas the deflection-based methods are geared more towards the design simulation.

Both of these approaches have advantages and disadvantages. In general, the first method should yield more accurate results, at the expense of more complexity in calculation and modelling during the design process. These compromises are discussed in the next section.

For measuring material properties during construction, methods based on material characterization are more desirable. These methods have a distinct advantage because they can be combined with compatible laboratory tests to ensure that the properties specified during design are obtained during construction.

3. Definition of Moduli

As indicated in the previous section, one of the major parameters to be measured is the modulus of each layer. A question that often comes up is what type of modulus is measured with a particular method. In this section, an attempt is made to identify the nature of moduli measured with different methods. Since the focus of TxDOT is towards the moduli obtained with FWD or seismic methods, these two methods are elaborated more. Laboratory tests are becoming important. The role of laboratory moduli is also discussed.

The behavior of most soils and pavement materials under load can be represented by a stress-strain curve similar to the one shown in Figure 3.1. Three significant parameters related to this curve are:

1.   the initial tangent modulus, or maximum modulus (E_{max}) — the slope of the tangent to the curve passing through the origin,

2.   the strength of the material (s_{max}) — the horizontal line asymptotic to the curve, and

3.   the secant modulus (E_1, E_2 or E_3) — the slope of a line connecting the origin to any point of the curve.

The initial tangent modulus is directly affected by the stress state, and the density of the material. The secant modulus is strongly affected by the magnitude of strain experienced by the material.
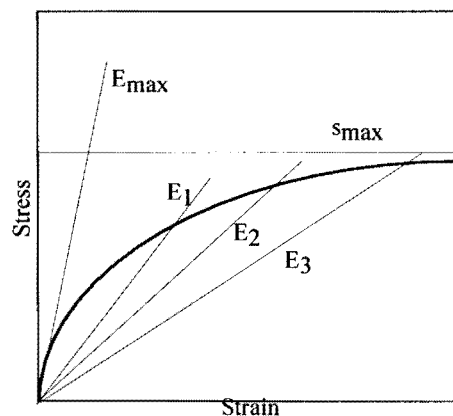
Figure 3.1 - Typical Stress-strain Curve for a Pavement Material

Since pavements, specially thin ones, may experience higher strains than those applicable to initial tangent modulus of a material, means of determining the secant modulus should be developed. To reasonably estimate the secant modulus, the stress-strain curve for each layer must be fully defined. From Figure 3.1, if a relationship between the initial tangent modulus and secant modulus can be developed, one can easily define the stress-strain curve. This is easier said than done for practical as well as analytical reasons.

Currently, the only reasonable way to develop the stress-strain relationship is through laboratory tests. The laboratory method of choice in pavement engineering is the resilient modulus (M_R) test. The resilient modulus test is time-consuming to perform, since a complete test on one specimen will take more than 4 hours. In addition, it is almost impossible to prepare specimens that are fully representative of the materials in the field (especially for bases). Other tests such as torsional shear resonant column are not included in this discussion since TxDOT does not own them, and since a high degree of expertise is required to perform them.

A number of parameters are used to define different types of moduli from different test methods. It would be beneficial to define these parameters first. Table 3.1 contains these terminologies.

In the M_R test, as reflected in Table 3.1, secant moduli at different confining pressures and deviatoric stresses are measured. After resilient modulus test is performed on a specimen, a mathematical model is fitted to the data. The recommended model at this time, based on a recent NCHRP project (Barksdale et al., 1994), is in the form of:

$$M_R = k_1 \, \sigma_d^{k2} \, \sigma_c^{k3}.$$ (3.1)

where σ_d and σ_c are the deviatoric stress and confining pressure, respectively. Parameters k_1 through k_3 are coefficients statistically determined from the results of the laboratory test. The accuracy and reasonableness of this model are extremely important because they are the key to successfully combine laboratory and field results.

The deviotoric stress is directly proportional to the axial strain, ϵ_{ax}, through:

$$\epsilon_{ax} = \sigma_d / M_R$$ (3.2)

By substituting Equation 3.2 in Equation 3.1, one obtains the following relationship:

$$M_R = K_1 \, \epsilon_{ax}^{K2} \, \sigma_c^{K3}.$$ (3.3)

Table 3.1 - Definition of Different Terms Used to Define Stiffness of Materials

Term	Definition
Resilient Modulus	The modulus of a pavement material determined in the laboratory from a variety of resilient modulus test protocols. This modulus normally corresponds to a secant modulus shown in Figure 3.1. Due to limitations with existing equipment in most cases it is difficult to determine the initial tangent modulus with the resilient modulus tests. Due to specimen disturbance, the moduli measured with this method are typically lower than field moduli. Research Report 1336-2F clarifies some of the sources of sample disturbance.
FWD Modulus	The modulus of a layer determined from the backcalculation of deflection basins measured in the field. This modulus normally corresponds to a secant modulus for materials close to the loading pad (i.e. AC layer, base and shallow subgrade) and an initial tangent modulus for materials far from the impact point (i.e. deeper subgrade materials).
Seismic Modulus	The modulus of a layer either directly measured or bakcalculated using a small seismic source. This modulus always corresponds to the initial tangent modulus since the impact is small.

The parameters are represented in uppercase in Equation 3.3 to emphasis that they are related to but are different from parameters k_1 through k_3 in Equation 3.1.

An alternative way of presenting the stress-strain curve shown in Figure 3.1 is through Equations 3.1 or 3.3. These graphs are included in Figure 3.2. From Figure 3.2a, the initial tangent modulus, E_{max}, correspond to the modulus at very small deviatoric stress, and is related to the confining pressure ($E_{max} = k_1 \, \sigma_c^{k3}$). The secant modulus at any other deviatoric stress (M_R in this case) can be found from the slope of the line. Figure 3.2b, which corresponds to Equation 3.3, provides the same information as Figure 3.2a, but in a more convenient way. In that figure, the secant modulus is directly related to strain. Once again, the initial tangent modulus is related to the confining pressure, and two of the parameters from Equation 3.3. The variation in secant modulus with strain on a log-log scale is a straight line.

It would be beneficial to plot the stress-strain curve for a typical material in Texas. Based on our experience, typical values of k_1, k_2 and k_3 (see Equation 3.1) for the base material in Texas are summarized in Table 3.2. We have also included the default values that are
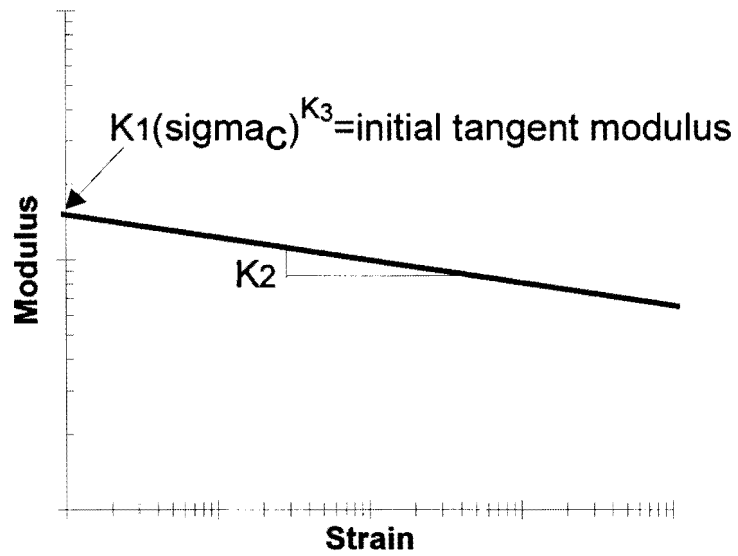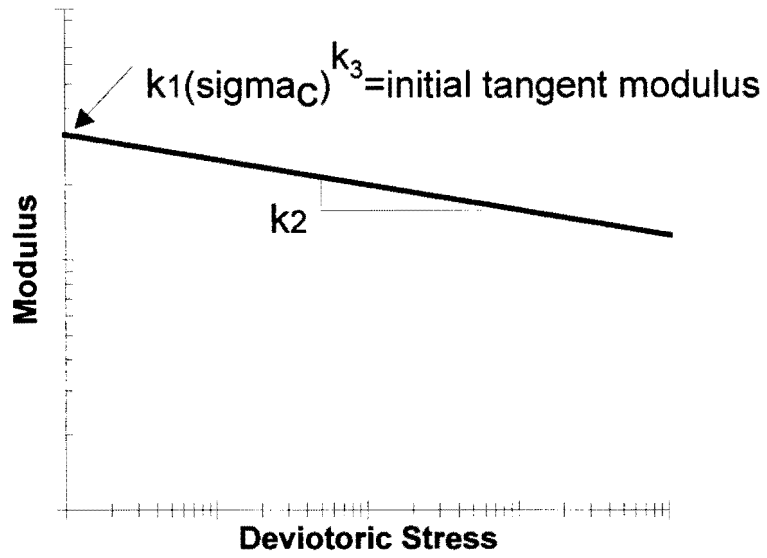
Figure 3.2 - Representation of Stress-Strain Curve
According to Equations. 3.1 and 3.3.

Table 3.2 - Typical Material Parameters Observed for Bases in Texas

Parameter	k_1 (KPa)	k_2	k_3	Confining Pressure(KPa)
Lower Bound	25,000	0	0.3	1
Upper Bound	100,000	-0.2	0.5	100
Default	50,000	-0.1	0.4	10

assumed for the future representations. The confining pressure varies from 1 KPa to 100 KPa to cover the range of confining pressures typically encountered in a pavement before and during loading.

Typical stress-strain curve for a base material in Texas is shown in Figure 3.3[1] for three different confining pressures. As the confining pressure (denoted CP on the figure) increases, the stress-strain curve moves upward, i.e., the modulus increases. However, as the strain increases, the secant modulus decreases.

To quantify these statements, the variation in modulus with strain using Equation 3.3 is shown in Figure 3.4. The minimum strain level shown is 10^{-4} percent which is considered as the threshold of the initial tangent modulus, E_{max}. The maximum of 1 percent strain is way above strain levels experienced by any functional pavement. Once again, as the confining pressure increases or the strain level decreases the modulus increases.

A convenient method to demonstrate the modulus versus strain curves shown in Figure 3.4 is to "normalize" them. To normalize the results, the modulus at a given strain and confining pressure is divided by the initial tangent modulus (in this case at a strain level of 10^{-4} percent) measured at the same confining pressure. Figure 3.5 reflects such a normalized curve where the results from the three confining pressures shown in Figure 3.4 collapse into one unique curve. The significance of this curve is that if one measures the initial tangent modulus for a given material, one can readily determine the modulus at any other strain level. This matter has significant practical and theoretical advantages that will be discussed later in the context of seismic and deflection-based moduli measured in the field.

Based on the extensive work in the area of geotechnical earthquake engineering (National Science Foundation, 1994), it is not unreasonable to assume that the values of k_2 and k_3 are

---

[1] default values from Table 3.2 are used in figures unless otherwise explicitly mentioned.
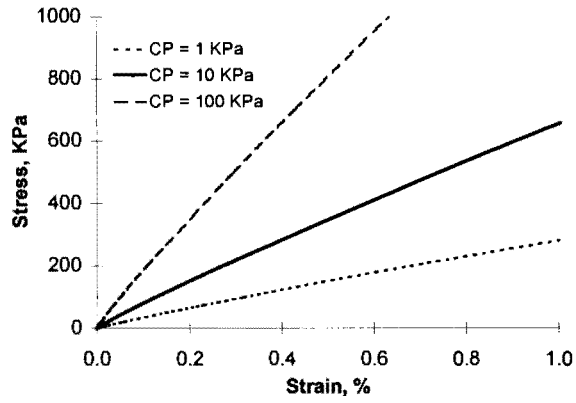
Figure 3.3 - Stress-Strain Curve for a Typical Texas Base
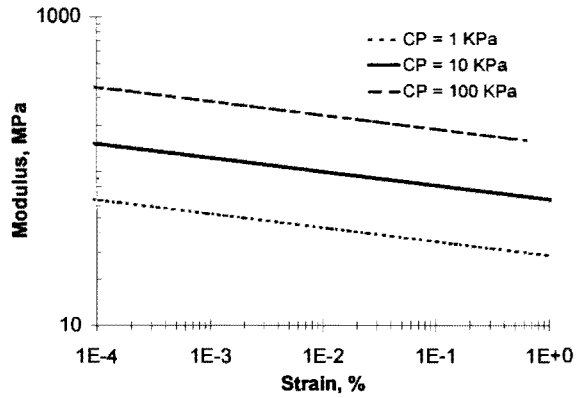
Figure 3.4 - Variation in Modulus with Strain for a Typical Texas Base
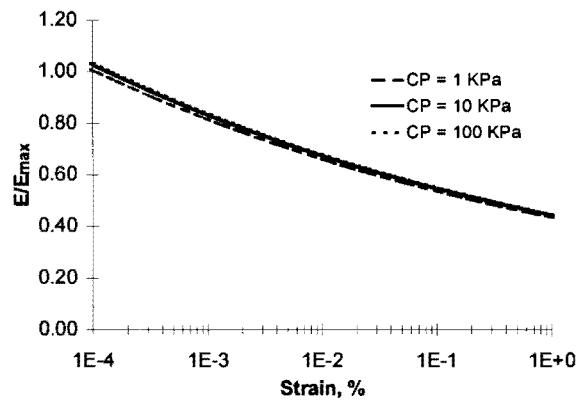
Figure 3.5 - Variation in Normalized Modulus with Strain for a Typical Texas Base

not very much affected by specimen disturbance, and as such can be determined from laboratory tests. However, the value of k_1 is extremely sensitive to sample disturbance, and should only be measured on an extremely high quality specimen (which is not practical to retrieve, especially for bases) or through field tests. The field tests of choice for practical use are FWD and SPA.

Let us assume that we construct a flexible pavement section with the material described above used as a base. For simplicity, let us assume that the asphalt layer has a thickness of 75 mm and modulus of 3.5 GPa. Also let us assume that the subgrade is a linear-elastic material with a modulus of 70 MPa. This pavement section is impacted by an FWD and a SPA.

FWD Tests. In the first exercise, the thickness of the base is varied between 100 mm to 300 mm. The variation in base modulus with depth is shown in Figure 3.6a. In all three cases, the moduli are not constant and decrease with depth within the base. As the thickness of the base increases, the moduli decrease. This happens because for thinner bases both the confining pressure and strain levels increase. As indicated before, an increase in confining pressure results in an increase in modulus. Inversely, the modulus decreases as the strain increases.

In Figure 3.6b, the depth within the base layer is normalized with respect to the thickness of the base (t_2) for convenience in superimposing the results. The modulus at mid-depth of the layer decreases as the thickness of the layer increases. But, the variations along the height of the base layer become more significant as the layer becomes thicker. For a 100-mm thick base, the modulus vary from about 220 MPa to 250 MPa, for a 200-mm thick layer from 260 MPa to 190 MPa, and for a 300-mm thick layer from 275 MPa to 165 MPa. Such variation will affect the deflection basin as well as the critical stresses and strains obtained for the design of pavement.

To assess the impact of the variation in modulus with depth in the base layer on the deflection basin measured with the FWD, deflections at seven points each 300 mm apart were determined under the following conditions:

1. the deflection basin was determined from a nonlinear layered model (Nazarian et al., 1996) which considers the constitutive model of the base as described in Equation 3.1. This deflection basin, which corresponds to the "actual" deflections measured in the field, is labeled as "nonlinear" in Figure 3.7.

2. the modulus of base at the mid-depth in Figure 3.6 was input into a linear-elastic layered model. The deflection basin labeled as "average linear" in Figure 3.7
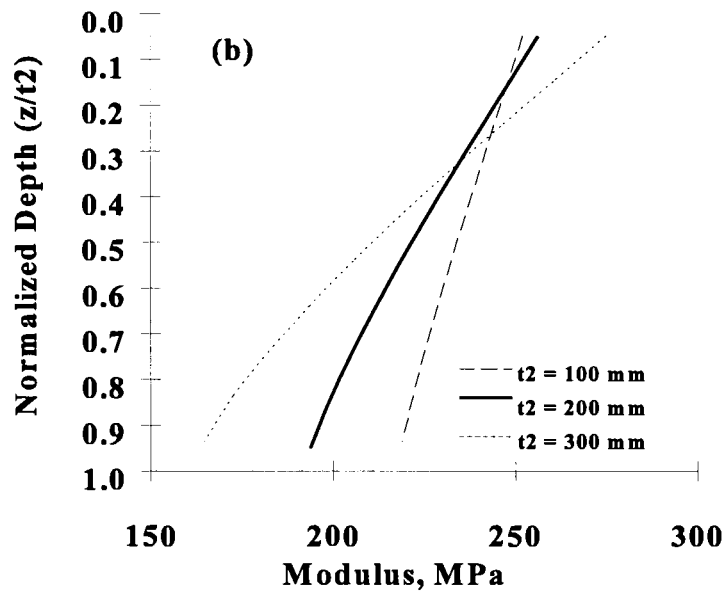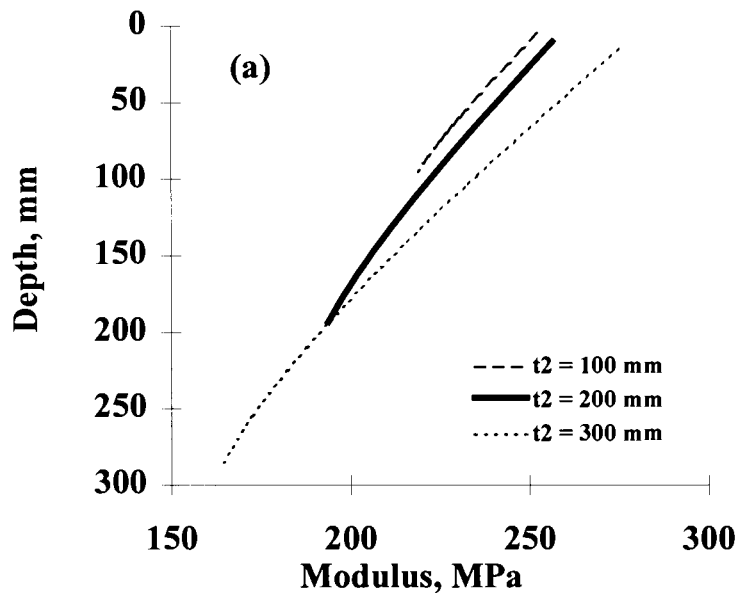
Figure 3.6 - Variation in Modulus of Base with Depth for Different Base Thicknesses
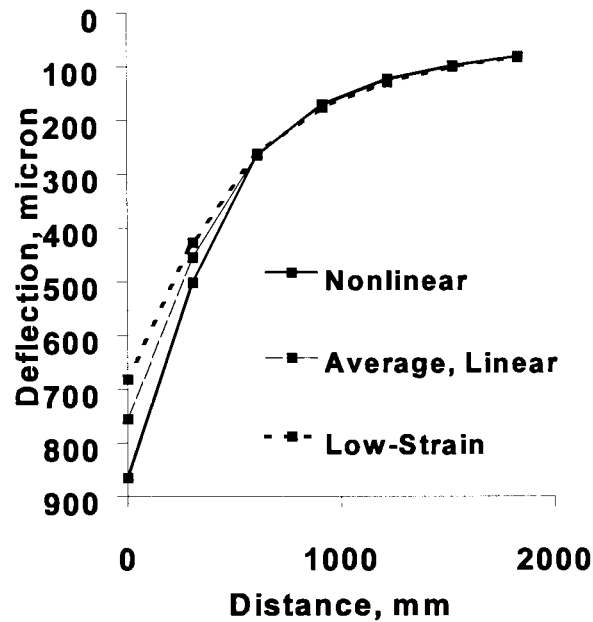
Figure 3.7 - Comparison of Deflection Bowls Measured with Different Moduli

corresponds to this set of data. This deflection basin can be considered as the "equivalent-linear" model used in design and analysis.

3. the confining pressure corresponding to the mid-depth of base in Figure 3.6 was used to determine the low-strain modulus of the base (see Figure 3.2). The deflection basin from that modulus input into a layered elastic program provides the deflection basin marked as "low-strain" in Figure 3.7. This condition should correspond to the condition when the linear elastic modulus from say SPA is used in the analysis or design.

Since the modulus of the AC and subgrade were assumed to be the same in all three cases, the deflection basins compare favorably for distances greater than 600 mm (see Figure 3.7 and Table 3.3). However, the deflections for the two sensors closest to the load differ from one another.

Any backcalculation (either with the FWD or the SPA) brings in some elements of non-uniqueness and uncertainty in the discussion. As such, we decided not to perform any type of inversion in this report. However, to assess the effects of the constitutive model on the final remaining life of a pavement, the critical strains under a standard dual-tandem load

Table 3.3 - Comparison of Critical Strains and Remaining Lives from Different Models

Parameter		Model Assumed		
		Nonlinear	Average Linear	Low-Strain[*]
Tangential Strain, micro-strain (bottom of AC)		361	281	225
Compressive Strain, micro-strain (top of Subgrade)		784	558	455
Remaining Life (1000 ESAL's)	Rutting	110	500	1,250
	Fatigue Cracking	231	525	1,090
Deflection Under 40 KN of FWD Load, micron	D1	865	755	681
	D2	501	454	426
	D3	265	263	262
	D4	169	172	176
	D5	122	125	128
	D6	97	99	99
	D7	80	81	82

* Not corrected for appropriate strain level due to wheel-load

were calculated. The results are summarized in Table 3.3. Depending on the assumption made significantly different strains are calculated.

The strains from the linear elastic model are the smallest, since the modulus of the base is the highest. The reason and conceptual remedies for this case will be offered later when the SPA tests are discussed. The strains from the "average linear" case are also smaller than the nonlinear case, indicating that for this example this approach may not be as conservative as the "actual" nonlinear case.

The remaining lives determined using Equations 2.1 and 2.2, as shown in Table 3.3 are vastly different. Compared to the nonlinear case, the rutting remaining life is over-estimated by about 5 times and 11 times for the average-linear and low-strain cases, respectively. The fatigue life is also overestimated by 2 to 4 times. Even though not shown here, as the base

layer becomes thicker the differences between the "nonlinear" and "average linear" become more pronounced, whereas the differences between the "nonlinear" and "low-strain" results become less significant. This happens because the low-strain modulus of the base changes slightly for different base thicknesses, whereas the modulus from the average linear changes more rapidly. It is obvious that this matter has significant implication in the analysis and design of pavements. We will discuss these implications further in a later section.

In Figure 3.8 the conceptual mechanism involved in characterizing the base layer under the FWD is depicted. Before the pavement is impacted, the confining pressure (CP1) and deviotoric stresses (or strains) are very small, and only due to gravity. Due to impact, the confining pressures (CP2) and deviotoric stresses increase significantly to the region enclosed by an oval. Three data points are shown in Figure 3.8, near the top of base, at mid-depth, and near the bottom of the base. Since the confining pressure and deviotoric stress are related, for each point they decrease and increase relatively proportionally. These differences in stress result in the variation in modulus within the layer.

In Figure 3.9 the variations in modulus with confining pressure and deviatoric stress for two different base materials are shown. In this case, the two materials have the same low-strain modulus before FWD loading. However, since the parameters k_1, k_2 and k_3 are vastly different for the two materials, the modulus at mid-depth will be different. Therefore, it would be difficult to correlate the modulus from the FWD and the laboratory. However, they can be combined if necessary.

SPA Tests. The conceptual way of representing the seismic moduli is simple. Referring to Figure 3.1, the moduli measured are the initial tangent moduli which always lie on the y-axis in Figure 3.2b. Therefore, of the three k parameters in Equation 3.1 or 3.3 only k_1 and k_3 play a role. This implies that in Figure 3.8 and 3.9 the state of stress before and after the SPA loading are very similar and equal to the point marked as "Before FWD Testing". Theoretically speaking, one can all but combine the effects of k_3 and k_1 in one parameter as shown in Figure 3.2. Practically, this point is true if one only is interested in determining the low strain modulus of the material, without using the results in design process. Once again, laboratory tests are necessary to determine the k parameters for design purposes.

The impacts used in seismic tests are quite soft, and therefore, change the state of stress negligibly. As such, the confining pressure under seismic tests are directly related to the overburden pressure, and its variation before and after tests is almost negligible. This implies that the variability in the modulus of base experienced under FWD loads does not occur during seismic tests.
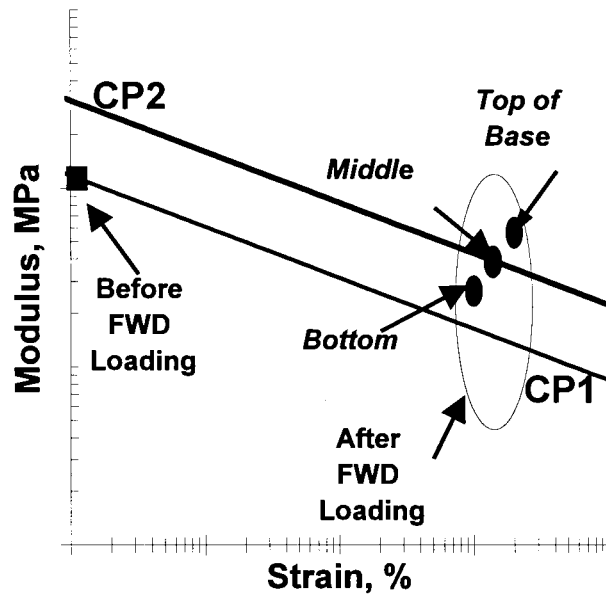
Figure 3.8 - Schematic of Conceptual Mechanism Involved in Characterizing Typical Base Modulus under FWD Load
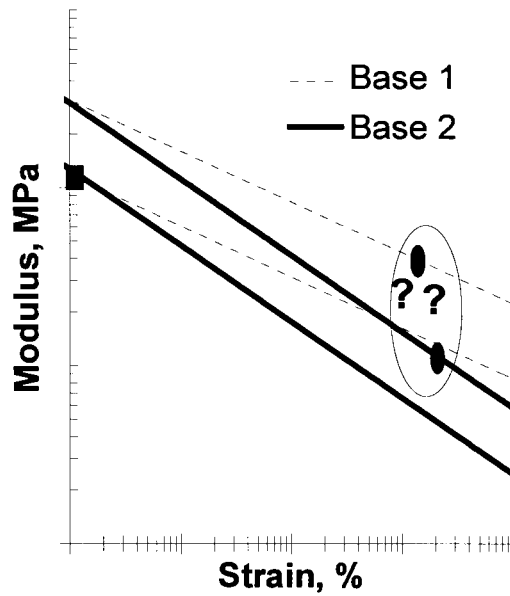
Figure 3.9 - Impact of Material Constitutive Model on Typical Base Material

The following conclusions can be drawn from this parametric study:

- under the FWD loading a set of complex interactions between the confining pressure and deviatoric stress occur which affect the modulus of a layer, and its variation with depth.

- the so-called "average linear" solution, which correspond to the state of practice in TxDOT, may not in a close manner resemble the behavior of a pavement.

- the low-strain modulus is higher than those experienced under standard loading.

The practical implications of these conclusions are the following:

- even under ideal laboratory and field testing conditions, a simple correlation between the laboratory and FWD or SPA moduli is quite difficult to develop; however, relationships for a given material from one quarry may be possible.

- the low-strain moduli from SPA cannot be directly used in pavement design; a simulation software is needed to combine the laboratory model and field data for design.

- the backcalculation of the FWD moduli using linear-elastic layered model to determine the "average" property of the base layer may not yield accurate enough results; a nonlinear model combined with laboratory model should be used.

None of the practical shortcomings of the methods are included in this discussion. If these shortcomings are considered, the problem becomes even more complicated. The advantages and shortcomings of each method are summarized in Table 3.4. Typically, due to sample disturbance and problems related with the resilient modulus test setup, it is impossible to measure a k_1 value which is representative of the field condition. However, the values of k_2 and k_3 can be assessed from laboratory tests.

The FWD tests simulate the applied loads reasonably; however they suffer from non-uniqueness in the backcalculated moduli. In addition, as shown above, the use of a linear-elastic model in the backcalculation may not always yield satisfactory results. The potential dynamic effects due to depth to a rigid layer should also be combined.

The SPA tests also suffer from non-uniqueness in the backcalculated moduli. In addition, only small-strain modulus is measured. An algorithm that numerically simulate the loading

condition is necessary. Once again in this study the strain-rate effects are not considered (i.e. correction for the frequency at which the seismic modulus are measured should be applied).

The FWD is a versatile test that is used in today's design methodologies. In this process, each pavement layer is modelled as a uniform linear elastic layer. The "average-linear" (also known as the equivalent-linear) modulus as defined in Figure 3.7 is determined. However, as indicated in Figure 3.8, the modulus actually may vary within the layer due to load-

Table 3.4 - Advantages and Disadvantages of Methods Used to Obtain Moduli

Test Method	Major Advantage(s)	Major Weakness(es)
Resilient Modulus	. Valuable for developing constitutive model for a material (i.e., variation in modulus with the state of stress and strain)	. Very difficult to prepare specimens with the same characteristics of in situ materials . Time consuming and expensive to perform
Deflection Methods	. Covers a representative volume of material . Imposes loads that approximate wheel loads	. Accurate determination of moduli of pavement layers may be difficult due to problems with backcalculation . The state-of-stress within pavement strongly depends on moduli of different layers, and hence is unknown.
Seismic Methods	. Covers a representative volume of material . Measures a fundamentally- correct parameter (i.e., linear elastic modulus)	. State-of-stress during seismic tests differs from the state-of-stress under actual loads . Modulus profile may suffer from backcalculation process

induced nonlinearity. Table 3.3 shows the potential impact of ignoring this matter. To alleviate this problem the FWD backcalculation should be conceptually modified. Either each layer should be subdivided into several thin layers during backcalculation with existing algorithms, or a nonlinear model which considers k_1, k_2 and k_3 for each layer should be used. Given the fact that only seven deflections are available, both these suggestions are impractical. The other option is to perform laboratory tests to determine k_2 and k_3 for Equation 3.1 or 3.3. Then by using a nonlinear model backcalculate k_1. One should realize that this process will add another level of iterations to the backcalculation process.

Seismic methods do not measure and are not affected by parameter k_2. Therefore, laboratory tests should be performed to determine k_2 and k_3. Since seismic tests measure initial tangent modulus ($E_{max} = k_1 \sigma_c^{k_3}$), one can determine k_1 since confining pressure (σ_c) and k_3 are

already known. As a reminder, σ_c in this case is only due to the overburden pressure and can be easily determined from:

$$\sigma_c = (2k_o + 1) \sum \gamma \, h \tag{3-4}$$

where k_o is the coefficient of earth pressure at rest, γ is the unit weight of pavement material, and h is depth. Now since k_1 through k_3 are known, one can use a forward modeling approach to calculate moduli at any depth.

In summary, both seismic and deflection methods need to be combined with laboratory test results so that a more robust design algorithm can be developed.

4. Overview of Proposed Methods

As indicated before, three devices are under consideration in this study. These devices are:

- A modified portable Seismic Pavement Analyzer for rapid determination of modulus of AC, base and prepared subgrade.

- A dynamic cone penetration device will be retrofitted with appropriate sensors, so that the elastic modulus and Poisson's ratio of the subgrade can be determined relatively rapidly and with minimal disturbance.

- A combined deflection/seismic device

Each device is described below. However, the results of a search for existing alternative devices are described first.

Existing Devices and Concepts

The results of an extensive search provided little indication of any highway agency deviating from the standard methodologies used in the state of practice. However, three sources of emerging technologies were identified.

A dynamic plate load test has been prototyped at the Georgia Institute of Technology (Rix, 1996). Basically, a rigid plate is struck with an instrumented hammer. The deformation of the plate is measured with two geophones. Through a simple dynamic analysis, a low-strain modulus of the pavement system is determined. This test is similar to performing FWD tests with one sensor. Alternatively, the Impulse Response test performed by the SPA can be used to obtain similar results. The device does not provide layer specific parameter, but an overall stiffness.

In the 1997 Transportation Research Board Annual Meeting, Linveh et al. (1997) presented the development of a portable FWD device. The device, which contains a drop hammer and a sensor, conveniently and automatically measures the load and deflection of the pavement system and reports an equivalent modulus. This device, similar to the previous one, provides an overall modulus and is not layer specific.

Along the same lines, a system with similar features as the ones described by Rix or Linveh et al. was exhibited at the TRB Annual Meeting. We have not received technical information about the device as yet. However, as we understood from the description of the vendor, the device consists of a vibrator and a receiver. Once again, the device measures load imparted

by the vibrator and determines the deformation by the receiver. Through an elastic wave analysis, the modulus of the system is determined. At this time we are awaiting more information from the vendor. We also volunteered to evaluate the device as soon as a beta prototype becomes available.

In summary, most highway agencies still use the density as a tool for quality control. There is a recognition by many entities that this may not be enough. However, no layer-specific tools are currently being developed.

Portable Seismic Pavement Analyzer (PSPA).

With the PSPA, the Young's and shear moduli of a certain layer are nondestructively measured by generating and detecting the arrivals of compression, shear or surface waves. The historical development as well as the theoretical and experimental background behind these tests can be found in Baker et al. (1995).

The PSPA is controlled by a computer. This computer is tethered to the hand-carried transducer unit through a cable that carries power to the accelerometers and hammer and returns the measured signal to the data acquisition board in the computer. The major mechanical components of the PSPA are depicted in Figure 4.1. These include the near and far accelerometers (A and B), the electric solenoid used as a source (C), the amplifier board (D), the solenoid firing board (E), and the computer system (F). The main structural member holding the transducers and source is a thick steel plate mounted to the base of the box holding the electronics. Rubber vibration isolators decouple the accelerometers (A and B) from the steel plate above 100 Hz. The source is directly mounted to the steel plate.

The reduction of data can be performed either in the time-domain or in the frequency domain. These processes are described below.

Time-Domain Data Reduction. In the time domain analysis, one relies on identifying the time at which different types of energy arrive at each sensor. The velocity of propagation, V, is typically determined by dividing the distance between two receivers, ΔX, by the difference in the arrival time of a specific wave, Δt. In general, the relationship can be written in the following form:

$$V = \frac{\Delta X}{\Delta t} \qquad (4.1)$$

In the equation, V can be the propagation velocity of any of the three waves [i.e. compression wave, V_P; shear wave, V_S; or surface (Rayleigh) wave, V_R].

Bottom View

S R

R R

Computer

A/D Board

Side View

End View

R R

R R S

R = receiver
S = source
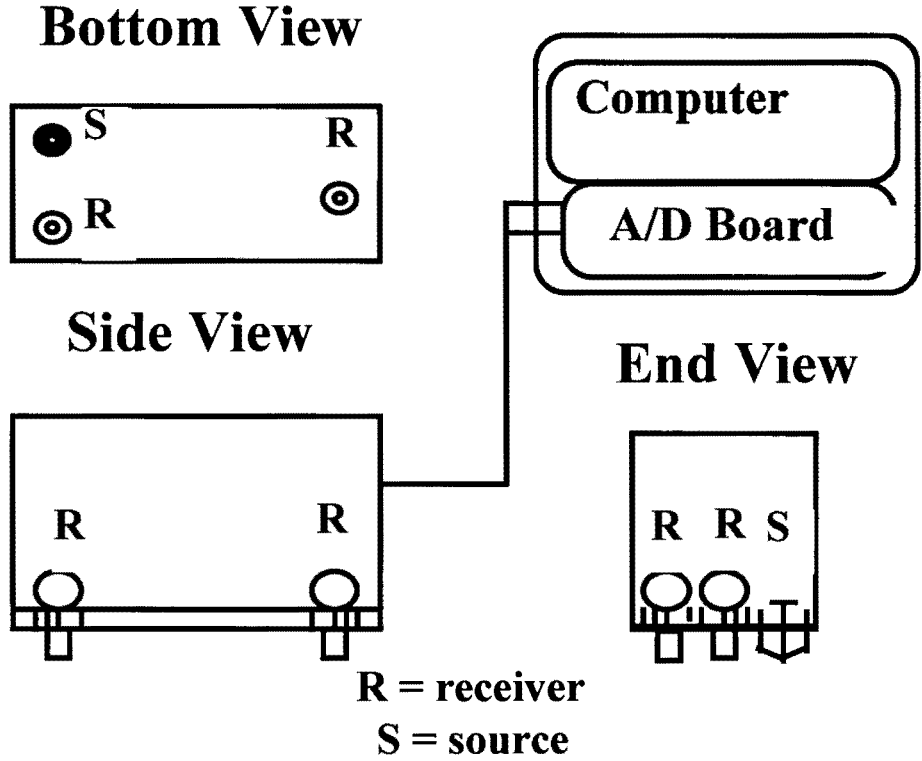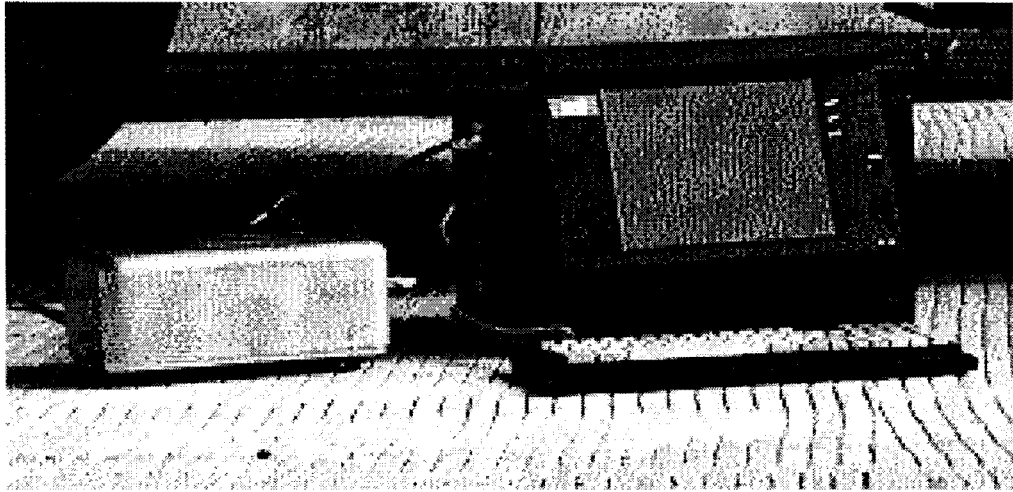
Figure 4.1 - Schematic of Portable Seismic Analyzer

Knowing wave velocity, modulus can be determined in several ways. Young's modulus, E, can be determined from shear modulus, G, through Poisson's ratio (v) using:

$$E = 2 (1 + v) G \qquad (4.2)$$

Shear modulus can be determined from shear wave velocity, V_S, using:

$$G = \frac{\gamma}{g} V_S^2 \qquad (4.3)$$

To obtain modulus from surface wave velocity, V_R is first converted to shear wave velocity using :

$$V_S = V_R (1.13 - 0.16v) \qquad (4.4)$$

The shear modulus is then determined by using Equation 4.3.

Typical records from two sensors placed 75 mm and 225 mm from the point of impact are shown in Figure 4.2. The arrivals of compression, shear and surface waves in each record are marked on the figure. The compression wave energy is easy to identify, because it is the earliest source of energy to appear in the time record.

The shear wave energy is about one-fourth of the seismic energy, and as such, is better pronounced in the record. The practical problem with identifying this type of waves is that they propagate at a speed that is close to that of the surface waves. As such, the separation of the two energies, at least for short distances from the source, may be difficult.

Surface waves contain about two-thirds of the seismic energy. As marked in Figure 4.2, the most dominant arrivals are related to the surface waves, as such it should be easy to measure them. If a layer does not have surface imperfections, this method can be readily used to determine the modulus. However, surface imperfections affect the repeatability and accuracy of the results.

Frequency-Domain Data Reduction. Since most of the energy in a seismic wave train is carried by surface waves, one can take advantage of the signal processing and spectral analysis to develop a more robust methodology for determining the modulus. The method is called the Spectral-Analysis-of-Surface-Waves (SASW; see Nazarian et al., 1995).

The goal with the SASW method is to generate and detect surface waves over a wide range of wavelengths. The time records collected with the set-up described above are transformed
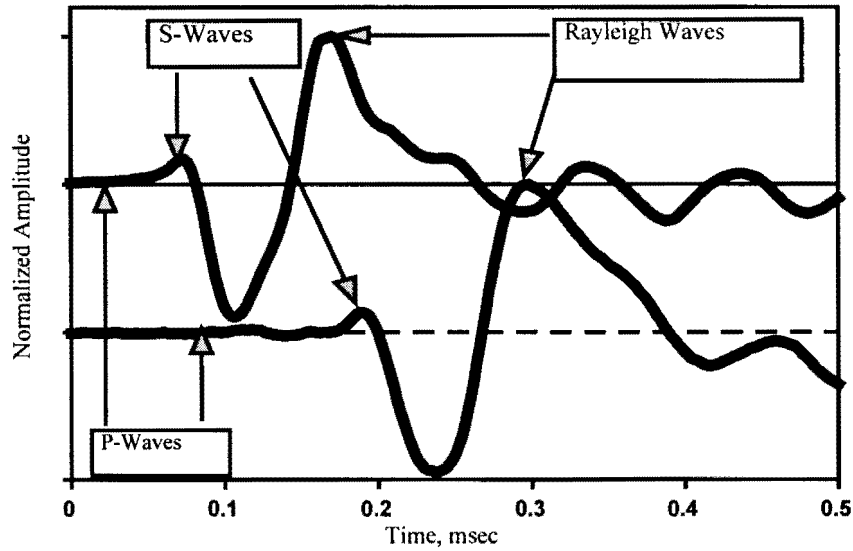
Figure 4.2 - Typical Time Domain from Portable Seismic Pavement Analyzer

to a so called dispersion curve — a plot of velocity of propagation of surface waves with wavelength. If the goal is to only determine the modulus of the PCC, the method becomes quite straight forward.

Consider the time records shown in Figure 4.2. By performing a fast Fourier transform on the two signals, and by dividing the two transformed signals by one another, one obtains a phase spectrum (i.e. variation in phase with frequency). Such a phase is shown in Figure 4.3a. In the first step, the phase is "unwrapped" as shown in Figure 4.3b. In the second step, a best fit line is fitted to the phase data for wavelengths shorter than the thickness of the PCC layer. As indicated by Baker et al. (1995), the slope of the line, m, can be directly related to Young's modulus, E, using

$$E = 2 \frac{\gamma}{g} (1 + v) [(1.13 - 0.16v) \frac{360 \Delta X^2}{m}] \tag{4.5}$$

where v is Poisson's ratio, and ΔX is the sensor spacing. As before γ and g are the unit weight and the acceleration of gravity, respectively.
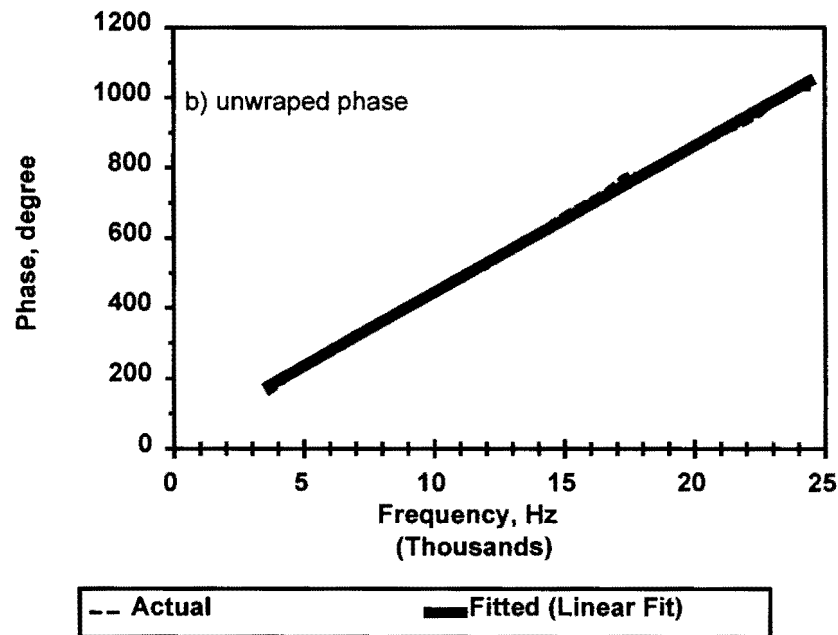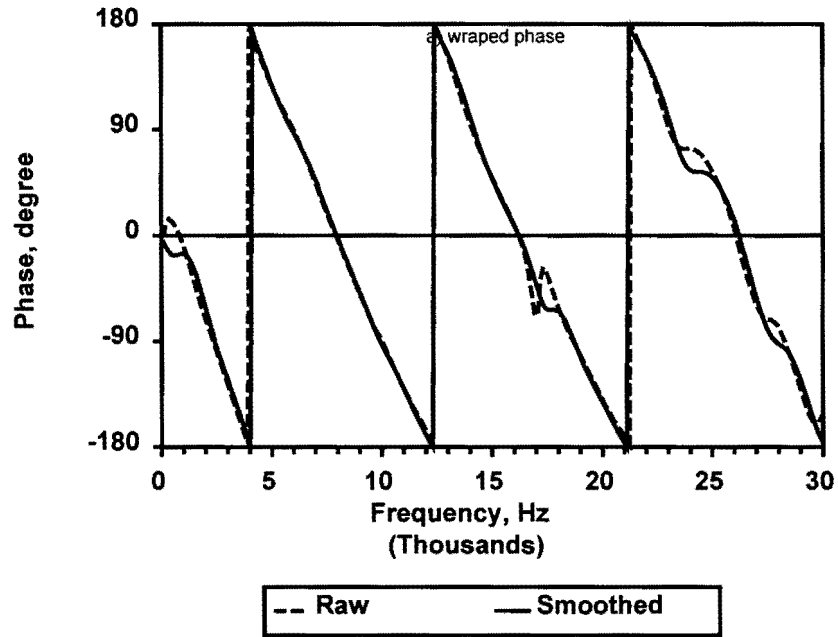
Figure 4.3 - Typical Data Reduction Process in the Frequency Domain for PSPA

Seismic Dynamic Cone Penetration Device

One of the tools that are typically used in the pavement engineering is the Dynamic Cone Penetrometer (DCP). In that test, a cone is penetrated into the ground under repeatedly impact loading. The rate of penetration (number of blows per mm) as a function of depth is an indirect measurement of the strength of a layer. This test can reasonably quantify the layers and qualify the type of material used. A three-dimensional accelerometer package will be retrofitted in the cone of the DCP to measure the modulus and Poisson's ratio as described below. Shinn et al. (1988) have developed a similar device but for deep geotechnical strata. The test proposed is nothing but a so called downhole seismic test (see Figure 4.4).

The schematic of downhole seismic tests is shown in Figure 4.4. The receivers are placed at the depth at which tests have to be performed. The pavement surface is then impacted with a small hand-held hammer. The records from the receivers are retrieved and saved for future analysis. The reduction of data consists of determining the arrivals of different waves
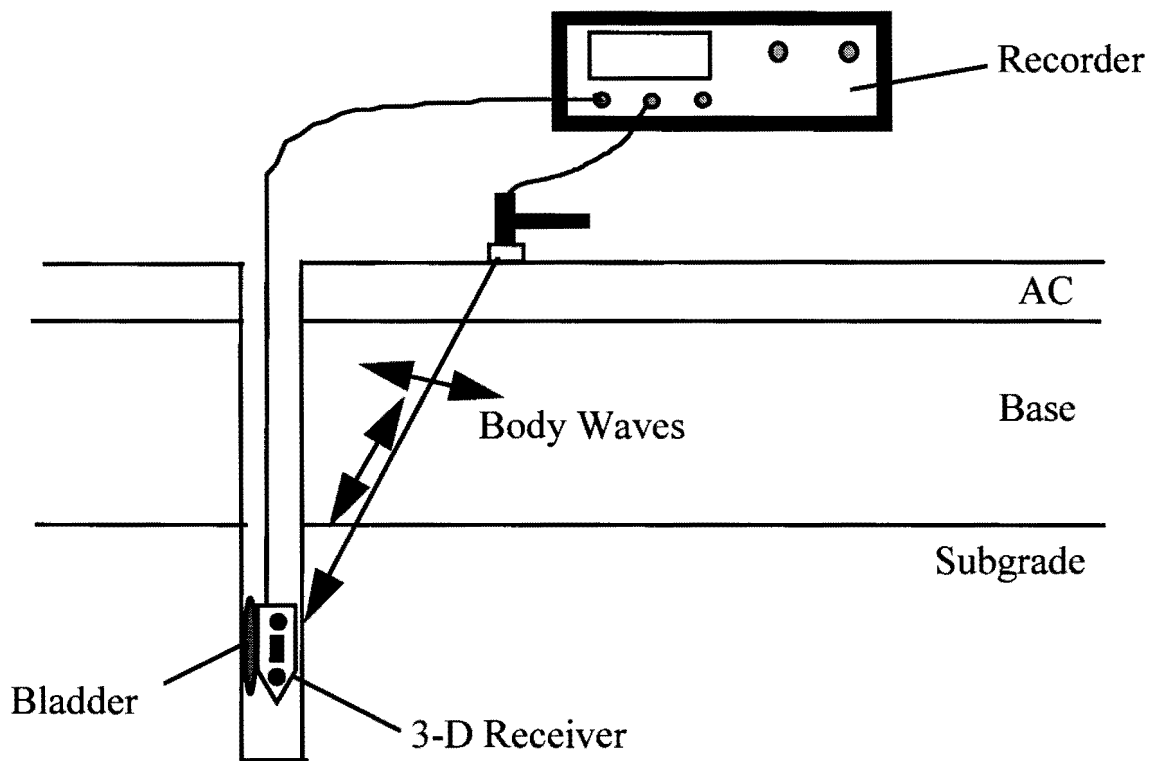
Figure 4.4 - Schematic of Downhole Seismic Tests

very similar to those carried out for the time-domain analysis of the PSPA. As soon as the velocities are calculated using Equation 4.1, the shear and Young's moduli can be determined using Equations 4.2 and 4.3. Once again if the shear and compression wave velocities are known, Poisson's ratio, ν, can be readily determined using:

$$\nu = \frac{0.5 \ \alpha^2 - 1}{\alpha^2 - 1} \tag{4-6}$$

where $\alpha = V_P / V_S$. (V_S and V_P are shear and compression wave velocities, respectively).

A typical time domain record from one Seismic DCP cone with a prototype device we have already developed is shown in Figure 4.5. The arrivals of the waves are clearly marked on the figure.

These tests are much more rapid than conventional downhole test. First, the DCP is used to install the borehole needed for placing the receiver with depth. In addition, it is possible to use the SPA source, data acquisition board and software to further accelerate the field test, and minimize cost.

Because of significant differences in the stiffness of different pavement layers, many experts prefer this method over other borehole tests because the possibility of generating refracted waves is very small for the downhole tests (National Science Foundation, 1994). Refracted waves complicate the interpretation of the results.

Combined Deflection-Seismic Device

This device at this time is under conceptual design, and is not available. However, it will be described for completeness.

Deflection-based methods, such as the Falling Weight Deflectometer (FWD), are the most common field evaluation device in Texas. The principles of the operation and the data reduction methodology for backcalculating moduli are well known and are not repeated here. Even though the device is an excellent tool for the day to day pavement evaluation, some researchers and practitioners have shown concern with respect to the moduli obtained with the device in certain conditions. The use of the device on top of the prepared subgrade may be difficult because of the magnitude of the load applied. The use of the device on top of the finished base is possible. However, the backcalculation of the modulus of base with the existing elasto-static models may be difficult because of large load-induced nonlinearity in

Time, msec
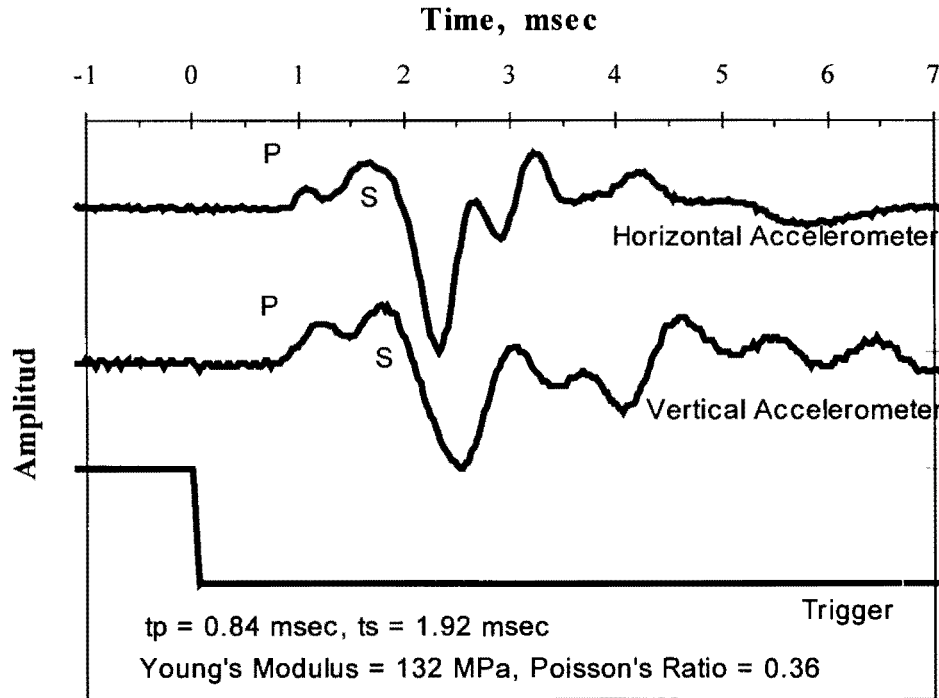
Figure 4.5 - Typical Time Records from DCP Tests

the material. In addition, the existence of shallow bedrock (or for projects that involve extensive cut and fill), the backcalculation methodology may not yield repeatable results.

Boddapati and Nazarian(1994) showed the importance of considering the pavement-FWD interaction. They indicated that for flexible pavements, the accuracy of the deflection from the first sensor is affected by the overall stiffness of the pavement. The more flexible the pavement (i.e. the thinner and weaker the AC and base) is, the less reliable the deflection of sensor 1 would be. The FWD impact plate cannot conform to the deformation of the pavement, and therefore, it cannot apply a uniform load to the pavement. The method is also not suitable for determining the modulus of thin AC or base layers.

Some of the short-comings mentioned above can be overcome in a manner that a deflection-based device can be used to estimate the stiffness parameters during construction. For example, the magnitude of the impact load can be reduced to minimize the plastic deformation of the base and subgrade, while at the same time maintaining the strain levels anticipated to occur under normal traffic loads. The loading period, which is typically about

30 to 80 msec, can be modified so that the deflections can be more sensitive to the properties of the top layers and less affected by the location of the bedrock. The problems with the plate-pavement interaction can be minimized by using much smaller contact area. Almost all these modifications require that the FWD impact be precisely controlled. Fortunately, the SPA has a computer-controlled source that can apply up to 700 KN (1500 lb) of load over a preselected duration. The diameter of the hammer is about 50 mm (2 in.) and overcomes the FWD-pavement interaction problem. Seismic method can potentially yield more accurate and comprehensive results with respect to the stiffness properties of paving layers. However, moduli are obtained at small-strains. By combining the FWD and SPA, the issue of strain and stress sensitivity of the material can be further studied. In addition, the results from the two methods can be combined to minimize the uncertainty of the moduli obtained for each layer.

UTEP, in cooperation with TxDOT and SHRP, has developed a trailer-mounted device called the Seismic Pavement Analyzer (see Figure 4.6). The details of the device are fully covered in UTEP Report 1243-1 (Nazarian et al., 1995).

Five different tests are carried out with the SPA and three with the PSPA:

1. Spectral Analysis of Surface Waves (SASW) (only with SPA),
2. Impulse Response (IR) (only with SPA),
3. Ultrasonic Body Wave (UBW) (with SPA and PSPA),
4. Ultrasonic Surface Wave (USW) (with SPA and PSPA), and
5. Impact Echo (IE) (with SPA and PSPA).

The SASW method is a seismic method that can nondestructively determine modulus profiles of pavement sections. A computer algorithm utilizes the time records to determine a representative dispersion curve in an automated fashion. The last step is to determine the elastic modulus of different layers, given the dispersion curve. An automated inversion process determines the stiffness profile of the pavement section. The method provides the modulus and thickness of different layers. With some modifications to the SPA and PSPA, the method can be applied after the completion of construction of each pavement layer. The fewer the number of layers, the more easily the moduli and thicknesses can be determined.

The ultrasonic-body-wave method can directly measure Young's modulus of the top layer. The ultrasonic-surface-wave method is an offshoot of the SASW method. The major distinction between these two methods is that in the ultrasonic-surface-wave method the shear modulus of the top layer can be easily and directly determined without a complex inversion algorithm. The results from these two methods can be combined to readily determine Poisson's ratio of the top layer.
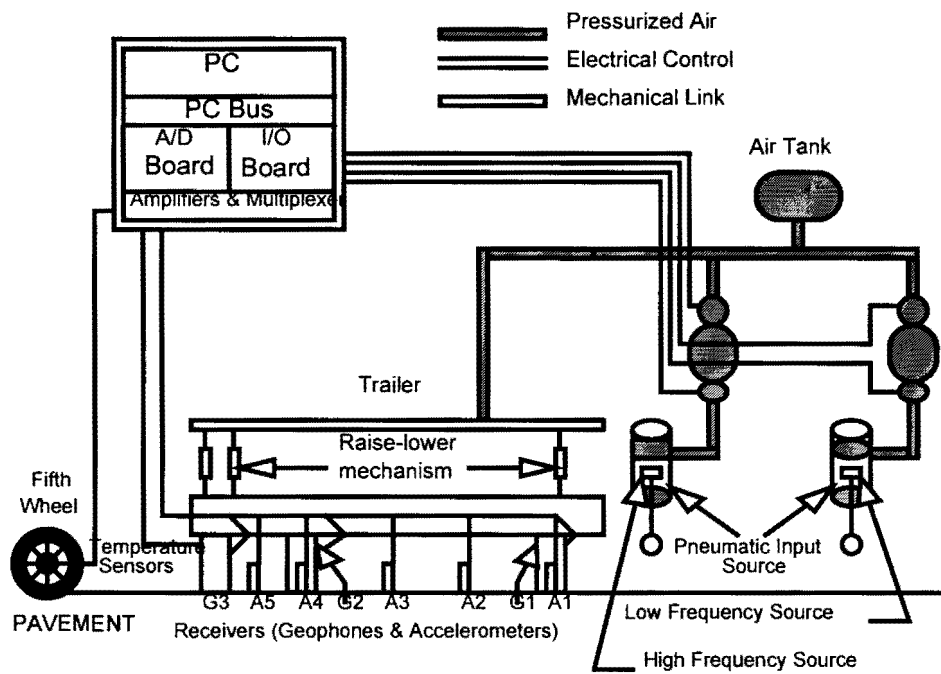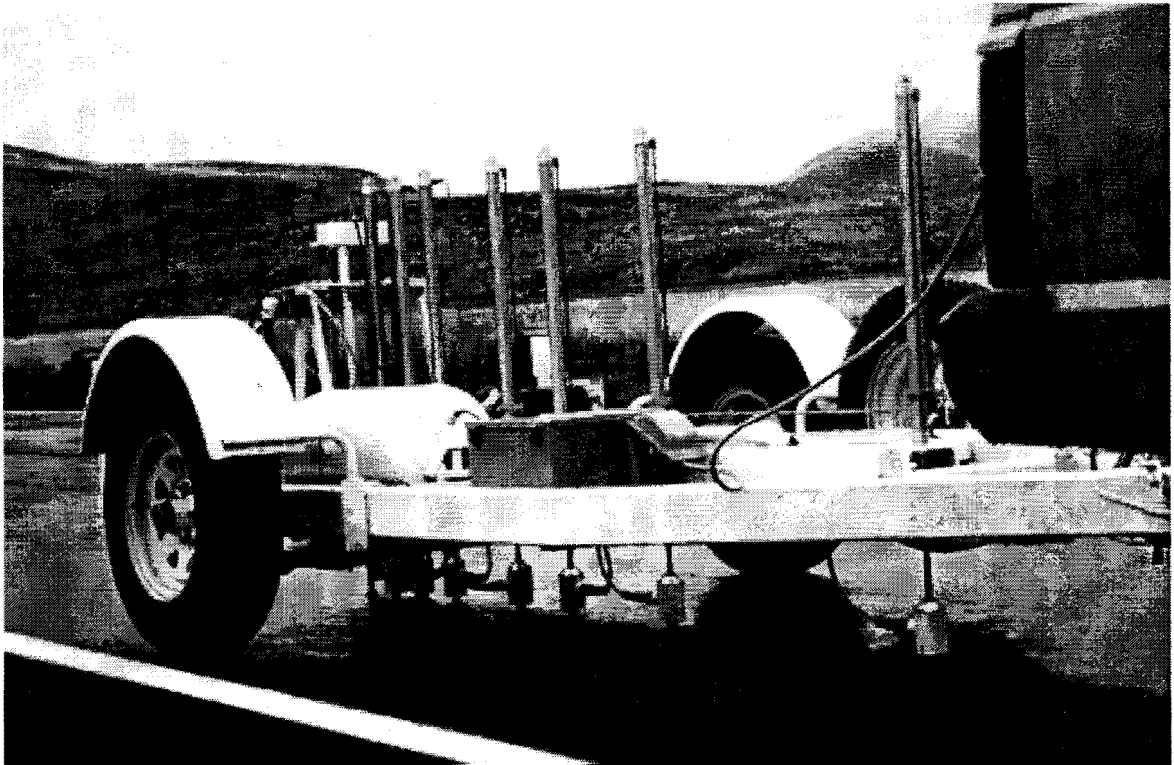
Figure 4.6 - Schematic of Seismic Pavement Analyzer

The impact-echo method can be used to determine the thickness of a thick AC layer as long as the layer is thicker than 10 cm.

The main parameter obtained on flexible pavements with the impulse-response (IR) method is overall stiffness of the pavement, which can be used to delineate between good and poor support. As a matter of fact this test is equivalent to performing FWD tests with only one sensor. It is quite possible to use the existing algorithms and apply them to a multi-sensor array to duplicate an FWD.

Other Tests

Other promising methods to consider is the Ground Penetrating Radar (GPR) for determining the thicknesses of layers. As indicated in section 2, thickness of different layers significantly impact the remaining life of a pavement. This method is being developed under a separate TxDOT project. It will be used in the future field tests associated with this project.

Operational Issues

One important aspect of a new device is the operational issues. These parameters are summarized in Table 4.2. The cost of each device vastly varies depending on the level that computer and data acquisition boards are shared between items. For example, a PSPA computer and data acquisition board can be used with several different sensor holders to test different components (i.e. AC, base and subgrade). In that case, the system would be fairly inexpensive. However, if a complete setup is needed for each layer, than the costs would be more. The measurement speed is set based on our experience with the SPA and PSPA , and the rate at which the traditional downhole tests are performed.

Traffic control is not necessary during construction. However, if the devices have to be used on a highway that is open to traffic, appropriate traffic control similar to those provided for the FWD should be available. All safety rules mandated by the State and Federal laws should also be observed.

Based on our experience with training several entities who operate SPA and PSPA, typically an initial two-day training course is necessary. The operators are then retrained after one month for an extra day on maintenance and judging the quality of data. The training for data reduction can also be done in the same manner.

Table 4.1 - Operational Issues for Devices

Parameter	Remarks		
	Portable SPA	Dynamic DCP	Combined Deflection/Seismic
Cost (1000 dollars)	20 to 30	9 to 20	90 to 130
Measurement Speed (minutes)	1	30 to 45	1 to 2
Traffic Control	Yes, if on existing pavement		
Skill Level of Operator	Consceincous Technician with three days of training		
Skill Level for Interpretation	Consceinous Technician with one week of training Engineer with one week of training		
Ambient Condition: AC	Temperatures less than 100°F	N/A	Temperatures less than 100°F
Ambient Condition: Base, Subgrade	No standing water	N/A	No standing water Material should be hard enough so that the source would not sink

Based on the PSPA and SPA operation, if the asphalt layer is extremely hot and viscous it would be difficult to propagate waves in them. For the base and subgrade the potential problem will be excessive moisture in the material. If the materials are extremely soft then the source may have coupling problems. This is one of the technical issues to be dealt with in this project.

The issues of repeatability and accuracy of the methods described above were extensively studied by Nazarian et al. (1993) during the development of the SPA. For the PSPA, we anticipate a repeatability of about 5 percent. This has been established based on our previous experience with the PSPA on PCC and AC layers. By repeating the test on a same point on a control slab, the coefficient of variation has always been less than 1 percent. Data from six different PSPA's have shown a difference of less than 3 percent. Therefore, the level of less than 5 percent should be quite reasonable.

For the combined seismic/deflection device, we anticipate a repeatability of about 5 percent for the top layer, 15 percent for base, and 10 percent for subgrade. These levels were established for the SPA during SHRP study, and are based on testing completed pavement.

For the seismic DCP we anticipate a precision of about 10 percent. This level has to still be verified; but based on our experience with the traditional downhole tests, it should be achievable.

By comparing these practical levels with the sensitivity levels defined in Table 2.4, one can conclude that these levels of precision are quite acceptable for tools being used for QA/QC of materials.

5. Case Studies

Several field case studies and several laboratory studies were carried out to determine the initial feasibility of suggested tests. The results are summarized here.

El Paso Case Study

A series of tests was carried out at a site near Horizon, Texas to determine the variation in modulus of base and subgrade with the PSPA. Besides seismic tests, a regular DCP and conventional nuclear density gauge were used. The typical cross-section consisted of 75 mm of ACP over granular base and subgrade. The granular base at the site was about 200 mm thick.

Typical seismic test set up is shown in Figure 5.1. Since an automated PSPA for base and subgrade is currently being built, tests were carried out by manually placing two accelerometers on top of the layer and impacting the surface with a hand-held hammer.

As indicated in section 4, test could be carried out and interpreted in the time or the frequency domain. Typical time domain records at one location from the base are shown in Figure 5.2. To determine the arrivals of the compression waves, the first excursion of energy has to be identified. These are marked as P in the figure. The arrivals of surface waves are also marked on the figure. These points, which are marked as R, correspond to the largest amount of energy in the records. From the differences in the arrivals of these two waves, Young's modulus and shear modulus are determined following the process described in section 4.

To reduce the data in the frequency domain, the phase spectrum between time records shown in Figure 5.2 is used. The phase spectrum from the base is shown in Figure 5.3. Following the process described in section 4, the modulus of the material can be obtained more robustly.

The variation in seismic modulus with location for the prepared subgrade is shown in Figure 5.4. A total of eleven points each about 2 m apart were tested. The results from the time-domain and frequency domain analyses are fairly close, and vary by a small amount. This occurs because the subgrade material was well compacted and did not contain large gravel. If a material does not contain fine cracks and surface imperfection the time-domain and frequency-domain analyses normally yield similar results.

The average moduli from the two methods are about the same and about 630 MPa. However, the moduli at most points are much less than the average value. The coefficient
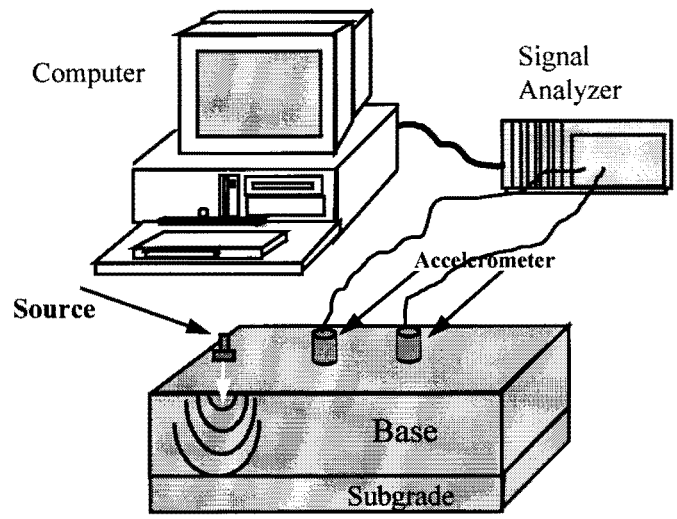
Figure 5.1. - Typical Test Set up Used in This Study
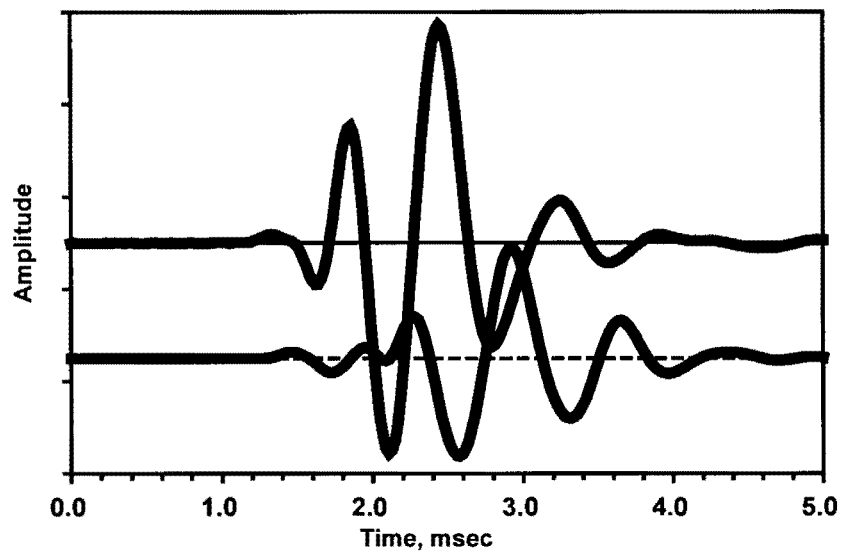
Figure 5.2. - Typical Time Domain Records from El Paso Study
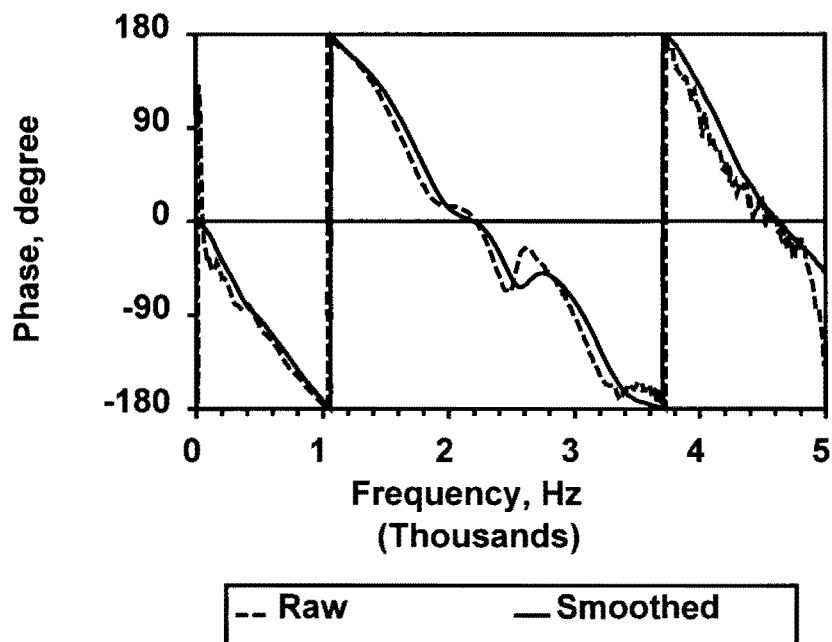
Figure 5.3 - Typical Frequency-Domain Results from El Paso Tests
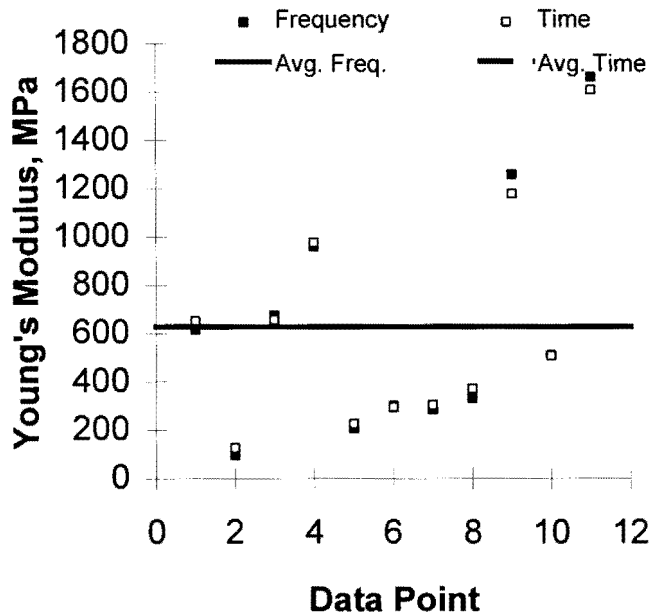
Figure 5.4 - Variation in Modulus along a Section of Subgrade in El Paso

coefficient of variation is about 70 percent, indicating large variability in the moduli. Such a large variability in modulus can be attributed to either the lack of precision of the method, or the actual material variability, or both.

A laboratory study was carried out to determine the repeatability of the seismic method. Six boxes, 1 m x 0.6 m were filled with the base material used at the Horizon site. The density and the moisture content were precisely controlled to be very close to the optimum. A 200 mm layer of base was placed in each case, four seismic tests were carried out on top of each material. The results from these tests showed that seismic tests are rather precise and repeatable at a level of about better than 7 percent. Therefore, the variation in modulus should be related to the variation in material properties.

In Figure 5.5 the variation in in-place dry density measured with a nuclear density gauge at six of the data points are related to seismic modulus. All points could not be tested because the nuclear device was needed for an ongoing project. A significant drop in modulus is associated with a small variation in dry density. Similarly, the variation in modulus with moisture content is shown in Figure 5.6. Once again, a mild correlation between the modulus and moisture content exists. We intend to pursue further these types of relationships in a laboratory environment as well as in the field.

$$E = 1137 \; DUW - 21822$$
$$R^2 = 0.61$$
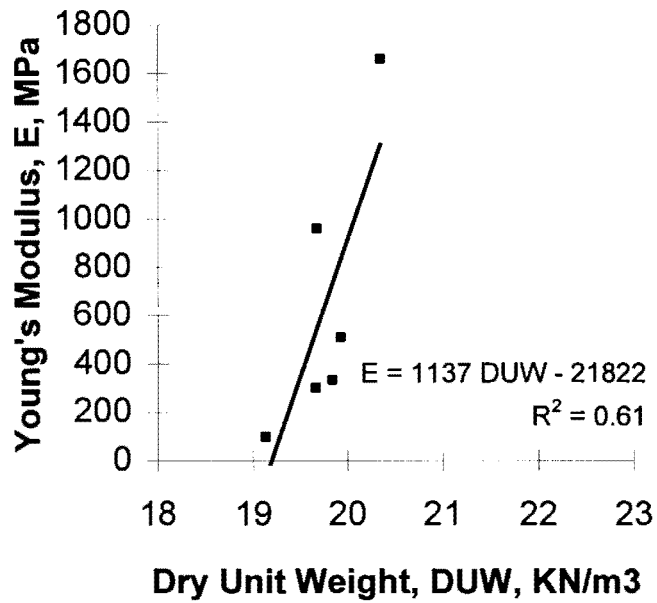
Figure 5.5 - Variation in Seismic Modulus with Dry Unit Weight for Subgrade Tested in El Paso

$$E = -746 \; MC + 7718$$
$$R^2 = 0.30$$
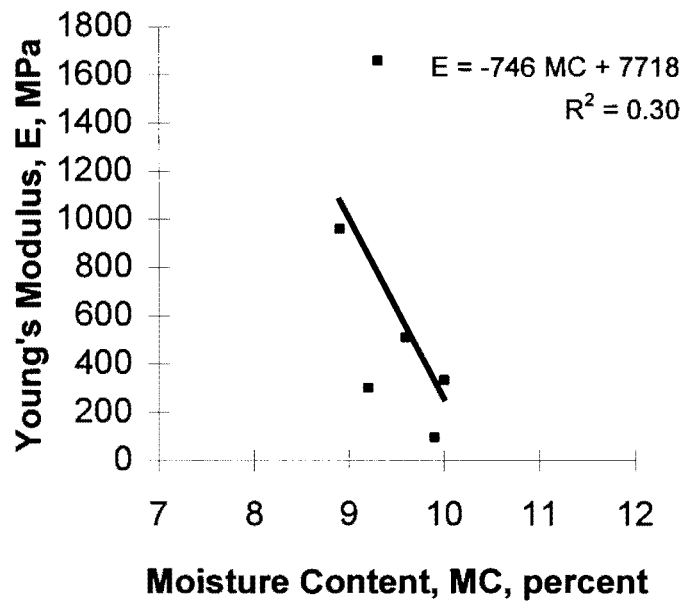
Figure 5.6 - Variation in Seismic Modulus with Dry Unit Weight for Subgrade Tested in El Paso

By measuring the shear and compression wave velocities, Poisson's ratio can be calculated (see Appendix A). The variation in Poisson's ratio with location, as shown in Figure 5.7, vary between 0.34 and 0.43. The average Poisson's ratio is about 0.39. Typically, the lower moduli coincide with higher Poisson's ratio (compare Figures 5.3 and 5.7). The higher Poisson's ratios are usually related to wetter subgrades.

Similar tests were performed on the base material about 1000 m away from the subgrade site. Once again, tests were carried out at 2 m intervals. The variation in modulus with test location is shown in Figure 5.8. Unlike the subgrade, some differences are evident between the results from the time and frequency domain analyses. These differences typically show up when the surface is course and microcracks are present at a site. Nazarian et al. (1997) clearly show that the time-domain results are not as reliable in these cases. The time-domain moduli are basically a bulk moduli which are seriously affected by the surface imperfections. Moduli measured with the frequency domain analysis is the average modulus over a range of thickness explicitly defined during the data reduction. We recommend the use of the frequency-domain analysis because, even though more complex to implement, it is by far more robust. The average modulus from the time domain is less than the frequency domain. This usually happens because the bulk wavelength of the signal may be longer than the thickness of the base.

The variation in Poisson's ratio along the length of the project, as shown in Figure 5.9, vary between 0.38 and 0.43. The reason for one outlier is not known at this time.

A comparison of different moduli related to this base is shown in Figure 5.10. The average seismic moduli is about 840 MPa with a coefficient of variation of about 23 percent. The resilient modulus of that type of base as measured in Project 1336 is about 470 MPa, which is about 80 percent less than the seismic modulus. As indicated in section 3, due to inherent problems with the resilient modulus sample preparation and set-up these levels of differences are anticipated. The seismic modulus using free-free resonant column test (se Appendix B) measured on laboratory specimens prepared to the average density and moisture of the base are about 745 MPa. However, when the specimens were prepared near the optimum water content as per Tex- 101 - E, the seismic modulus was about 227 MPa. These experiments indicate that the relationship between the field and laboratory compaction should be considered and addressed in this project.

DCP tests were also performed at the site. The relationship between CBR obtained from the DCP and seismic modulus is shown in Figure 5.11. The values of CBR reported correspond to the average value along the thickness of the base. Some scatter in the results can be observed. However, a trend towards greater CBR with greater modulus is apparent.
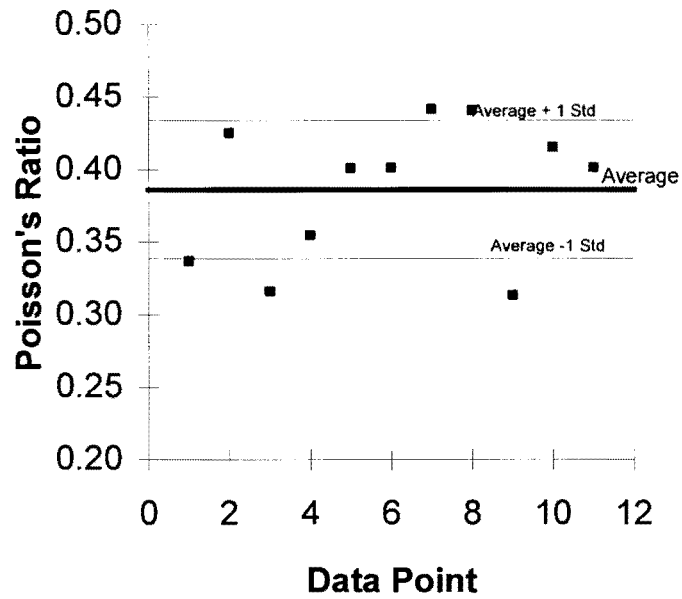
Figure 5.7 - Variation in Poisson's Ratio along Subgrade Tested in El Paso
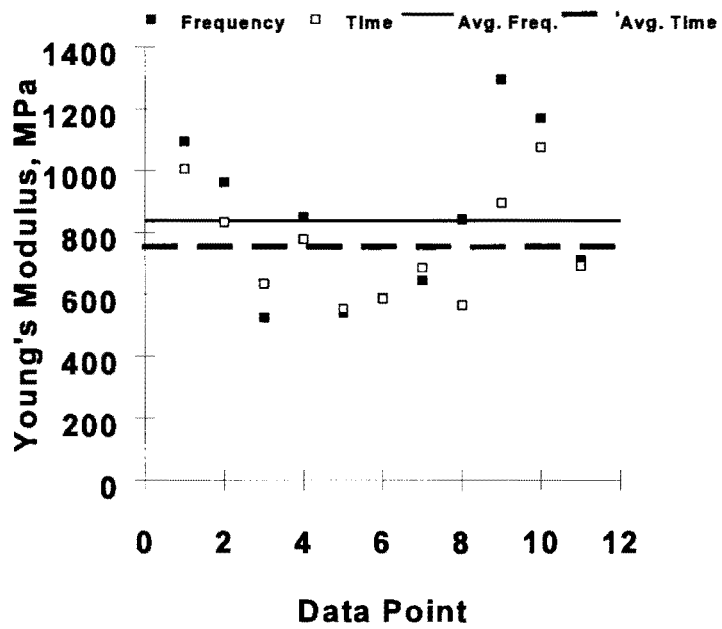
Figure 5.8 - Variation in Modulus along a Section of Base in El Paso
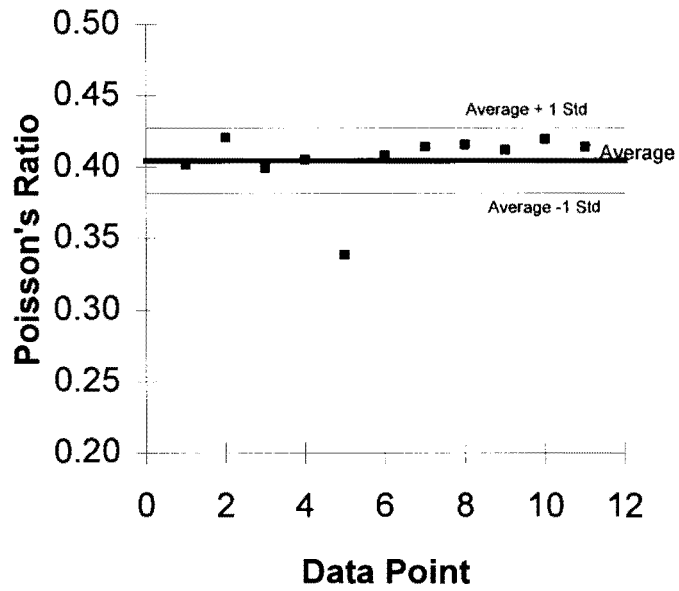
Figure 5.9 - Variation in Poisson's Ratio along Base Tested in El Paso
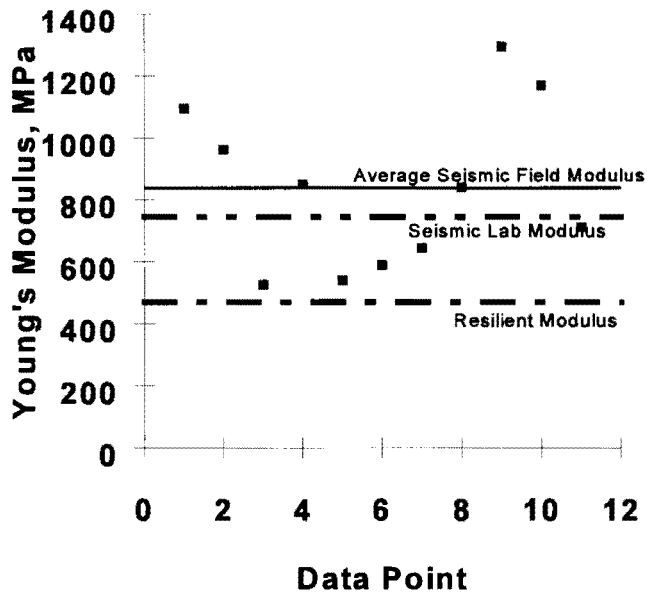
Figure 5.10 - Comparison of Moduli Obtained from different Methods on a Base Section in El Paso

The chart shows Young's Modulus, E, MPa (y-axis, 0 to 1400) versus CBR from DCP, percent (x-axis, 0 to 80) with scattered data points and a best-fit line, labeled:

$E = 15.84\ CBR$

$R^2 = 0.46$
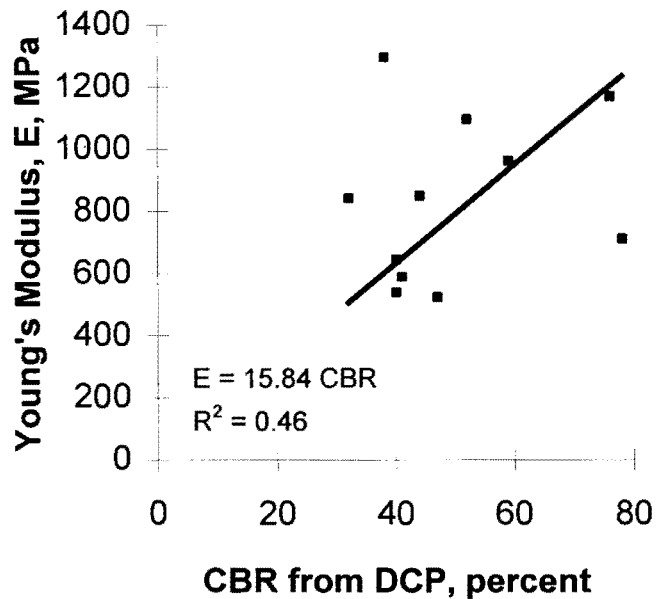
Figure 5.11 - Comparison of Seismic Modulus and CBR from DCP

Limitations of the seismic methods were discussed in section 4. Since a DCP tests are rather localized, some anomalies such as a larger gravel can influence the results. The best-fit line depicted in Figure 5.11, correspond to a ratio of about 2200 between the modulus and CBR, which is higher than 1500 suggested by AASHTO. However, it lies between the ranges of 750 and 3000 defined as reasonable in the AASHTO design.

The variations in seismic modulus with the in situ moisture content and dry density are included in Figure 5.12. Smaller modulus values are generally associated with higher moisture contents and lower dry densities. This trend seems reasonable however some scatter in data exists. The reasons for the scatter is not known at this time, and should be studied during the next 2.5 years of the project through laboratory and controlled field tests.

From this case study we learned that definite trends exists between field moisture content, density, CBR and seismic modulus. These relationships should be explored and described in more detail in the future. We also learned that specimens prepared as per Tex-111-E may yield moduli that are less than those measured in the field. However, if the laboratory specimens are prepared at the density and moisture level measured in the field, closer relationships between laboratory and seismic moduli can be developed.
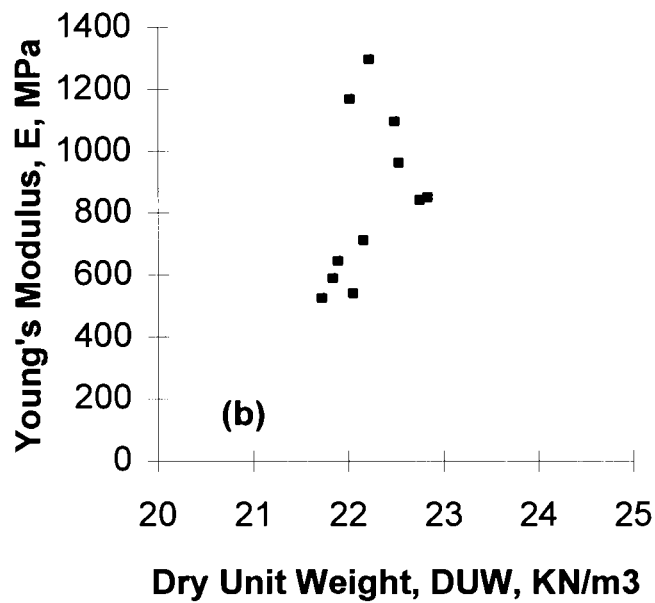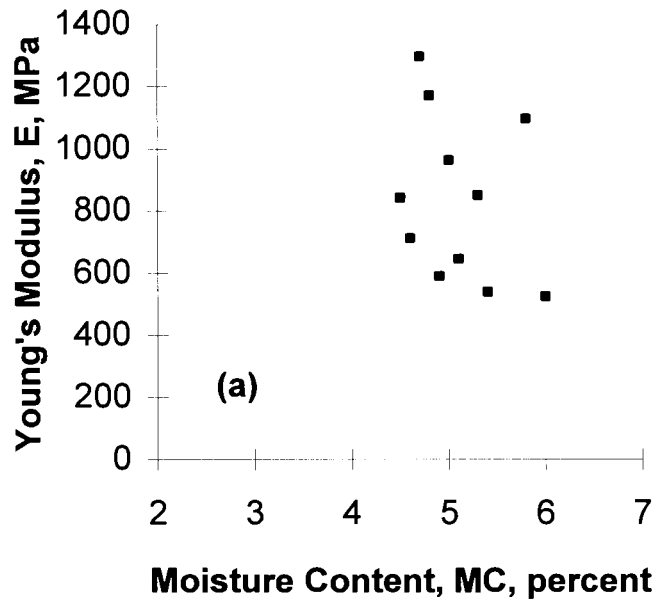
Figure 5.12 - Variation in Seismic Modulus with Moisture Content and Density of Base Materials at El Paso Site

Midland Case Study

The midland site was located on Loop 250 near Midland Municipal Airport. The pavement section at the site consisted of about 355 mm of base over subgrade. Seismic tests were performed on the subgrade as well as the base. The results along with other supporting information are described here. DCP tests were also performed during the base tests. However, in every single test (a total of 11 tests), the DCP could not be penetrated in the base more than 100 mm. Therefore, the values are not included here. FWD tests were also performed on top of the base. The results from the seismic and FWD tests are compared for completeness.

In Figure 5.13 the variation in modulus of subgrade at 21 points, each about 2 m apart, is demonstrated. The modulus of the subgrade for the first ten points are significantly lower than the last ten. Since the site was very close to the abutment of a bridge, we presume that the soil was not as thoroughly compacted at those location. On the other hand, the last ten points were heavily trafficked by construction equipment. Therefore, the trend seen in Figure 5.13 is quite reasonable.

The variation in Poisson's ratio with location is included in Figure 5.14. The first ten points (except an outlier), which were less compacted and wetter exhibit Poisson's ratios that are closer to 0.5; whereas, for the last ten points Poisson's ratios are smaller than average. Once again, a practical indication of reasonableness of the results. Since the site was covered with a layer of base as soon as our tests were completed no further information is available at this location.

To determine the moduli of base at this site, a location about 500 m away from the bridge was selected. Similar to the subgrade site, 21 points each about 2 m apart was tested. The variation in seismic modulus of the base at that location is shown in Figure 5.15. The modulus of base generally varies between 500 MPa and 1500 MPa with an average of about 1100 MPa. This indicates that the base is of high quality, as (at least qualitatively) suggested by the DCP tests. As indicated before, the DCP could not be penetrated into the base at all points tested.

Also shown in Figure 5.15 is the laboratory resilient modulus from a specimen compacted to the in situ condition and tested. The laboratory MR modulus is about half as much as the average field modulus — an expected trend.

The variation in Poisson's ratio of the base is shown in Figure 5.16. The average Poisson's ratio is about 0.35 with a standard deviation of 0.07. Three data points with low Poisson's
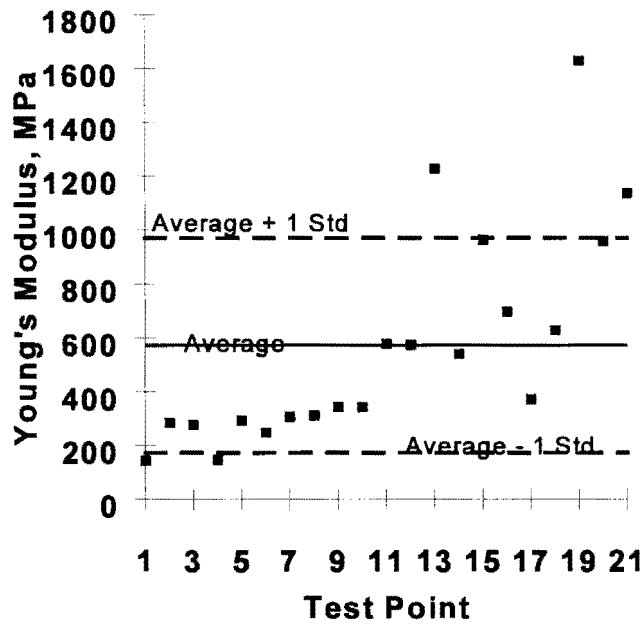
Figure 5.13 - Variation in Seismic Modulus of Subgrade from Frequency Domain Analysis at Midland Site
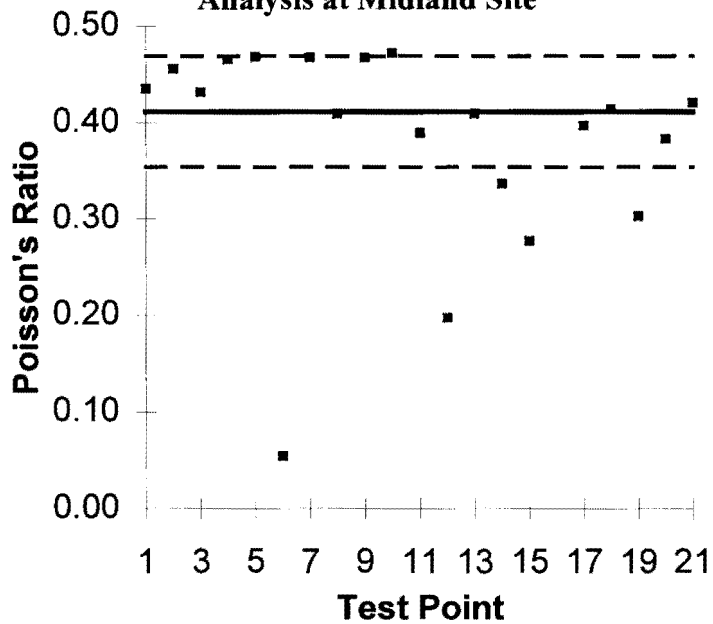
Figure 5.14 - Variation in Poisson's Ratio of Subgrade at Midland Site
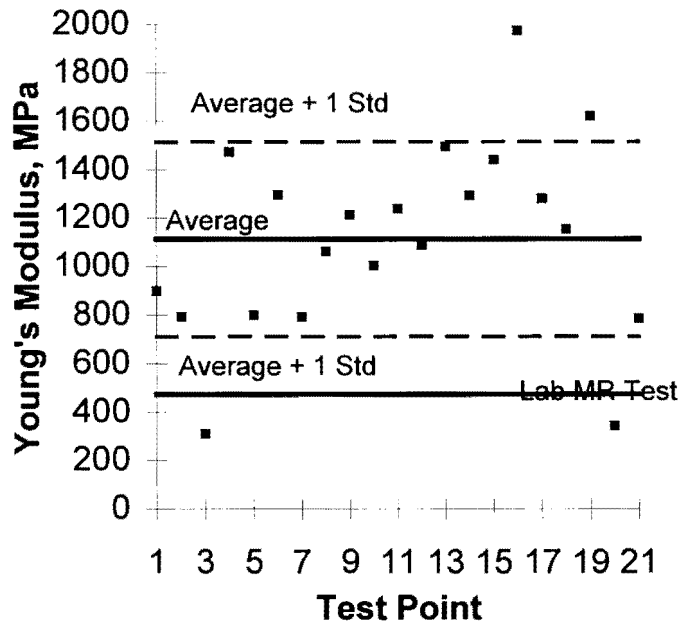
Figure 5.15 - Variation in Seismic Modulus of Base from Frequency Domain Analysis at Midland Site
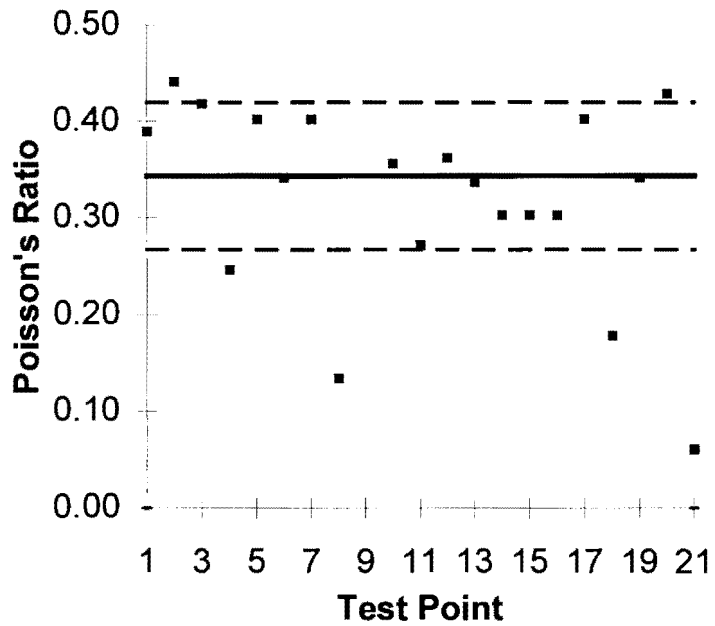
Figure 5.16 - Variation in Poisson's Ratio of Base at Midland Site
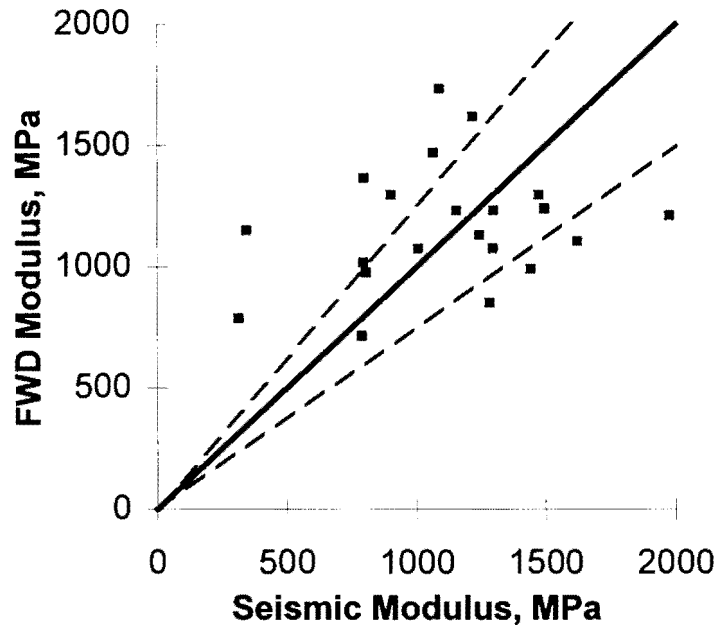
Figure 5.17 - Comparison of FWD and Seismic Modulus of Base at Midland Site

ratios can be seen in the figure. These can occur because of difficulties in consistently determining the arrivals of compression waves on some records.

The data from the FWD tests performed on the exposed base were also reduced. To obtain a reasonable match between the experimental and theoretical deflections during backcalculation, a 300 mm layer of subbase was arbitrarily assumed. Moduli measured with the seismic method are compared with the FWD moduli in Figure 5.17. Also shown in Figure 5.17 are the line of equality and lines corresponding to 25 percent variations from the line of equality. In this case most moduli are within 25 percent of one another. In our opinion such a close relationship is possible because the base was heavily compacted and was thick. Such close correlations may be more difficult for thinner and less stiff bases. However, the FWD tests should be evaluated in the future studies.

Odessa Case Study

A 45 m section of the access road of Highway 20 near Odessa District Office was tested with the SPA, FWD and PSPA. With the SPA and FWD the variation in modulus for different layers were obtained. The focus of the PSPA was the modulus of the AC layer. The pavement section at this site consisted of about 50 mm of AC over about 250 mm of base over subgrade.

The variation in seismic moduli of different layers along the road is shown in Figure 5.18. The moduli of subgrade at the nine points tested with the SPA were relatively constant with an average of about 250 MPa and a coefficient of variation of about 10 percent (see Figure 5.18a).

The base modulus is relatively constant with an average of about 550 MPa. As marked in Figure 5.18b, the laboratory resilient modulus performed on similar materials in Project 1336 provide a modulus of about 475 MPa for this layer, which is within a difference of 15 percent of the seismic modulus.

The modulus of AC layer is also relatively constant except for an area between 25 m and 35 m. This area coincide with the entrance to a closed business entity. The reason for lower moduli is not known at this time. On the average the modulus of the AC layer is about 13.8 GPa. Seven cores retrieved from this site were also tested in the laboratory using an ultrasonic device developed for Project 1369 (see Appendix B). The average modulus from the laboratory tests, as shown in Figure 5.18c is about 14.3 GPa. The close relationship between the laboratory and field numbers is of significance. Because the results of tests on laboratory brikettes can be directly translated into field results.

A comparison of the FWD and SPA moduli is included in Figure 5.19. The modulus of the AC layer was assumed to be constant for the FWD backcalculation because the layer was only about 50 mm thick. The dashed lines in Figure 5.19 bound a 25 percent variation from the line of equality. In general, moduli from FWD are higher than those from the SPA for the base, and lower for the subgrade. The lower moduli from the FWD can be attributed to the fact that the FWD samples deeper into the subgrade than the SPA.
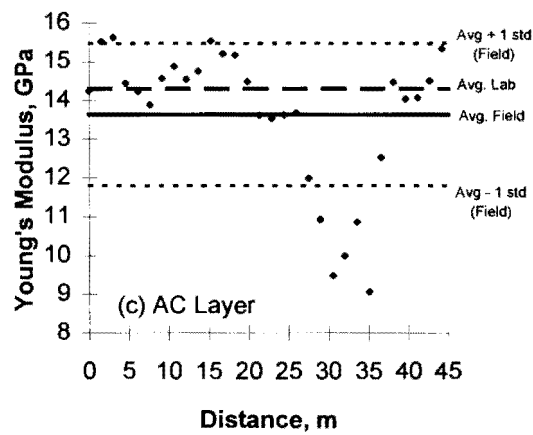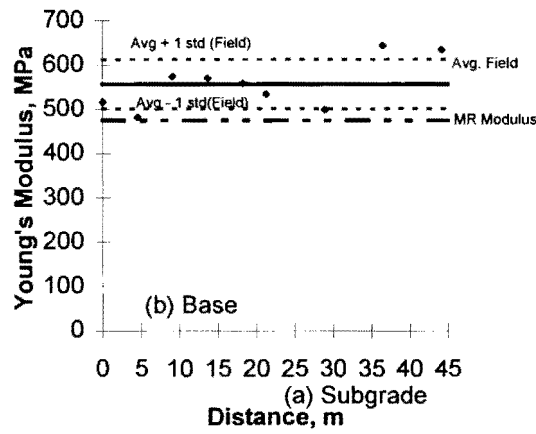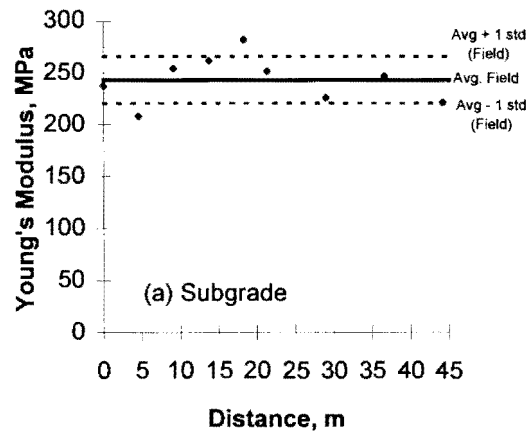
Figure 5.18 - Variation in Moduli of Different Layers at Odessa Site
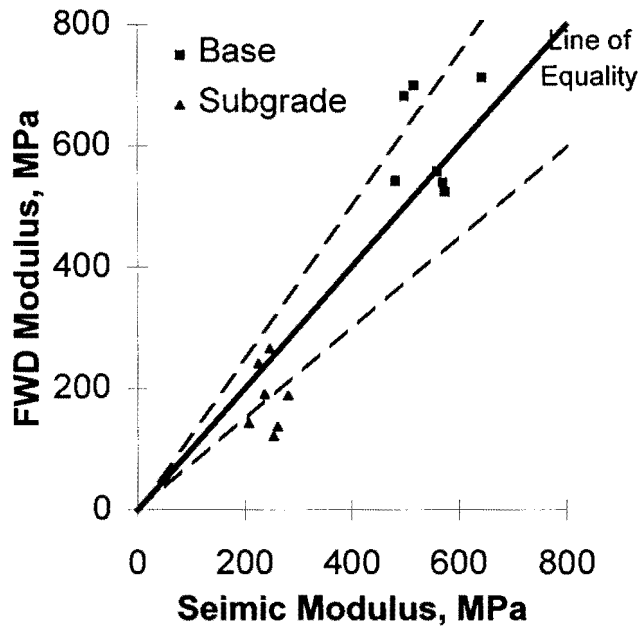
Figure 5.19 - Comparison of FWD and Seismic Moduli at Odessa Site

6. Summary and Conclusions

This report contains the initial feasibility study as well as technical and nontechnical issues related to developing equipment that can be used to measure the engineering properties of flexible pavement materials during construction.

The focus of this study is on the following three devices:

- A modified portable Seismic Pavement Analyzer for rapid determination of modulus of AC, base and prepared subgrade.

- A dynamic cone penetration device will be retrofitted with appropriate sensors, so that the elastic modulus and Poisson's ratio of the subgrade can be determined relatively rapidly and with minimal disturbance.

- A combined deflection/seismic device.

The main concentration of the study is towards seismic methods because of the following reasons:

- They measure a fundamentally correct property of the material (i.e. elastic modulus).

- In the most part, they can be duplicated in the laboratory; no other existing method has this capability.

Other equipment and procedures such as FWD, GPR will also be utilized.

A study was carried out to determine the engineering parameters that are important to the design of flexible pavements. Depending upon the thickness of different layers and mode of failure different parameters pay dominant roles. But in general the most important parameters are the thickness and moduli of different layers as well as Poisson's ratio of subgrade. These parameters should be measured fairly accurately.

A comprehensive discussion on the nature and role of moduli measured in the laboratory and with different NDT devices are also included. The relevance and ways of incorporating these moduli in design are thoroughly described. In general, results from any NDT test should be combined with laboratory results for realistic design.

The technical aspects of each test method suggested above, along with institutional and nontechnical parameters to be considered, are summarized. Most tests are relatively rapid

to perform, and depending on the level of sophistication devices will cost between $10,000 to $100,000. They all require short period of training for performing the tests with these devices, and a longer term training for interpreting the results.

Several case studies are included to show the level of sophistication in data collection, typical outcome from tests, and correlation with conventional methods. The following lessons learned from these case studies which should be thoroughly studied in the remainder of this project:

- Laboratory tests show that seismic tests are rather repeatable with a repeatability of better than 90 percent.

- In the field, the seismic modulus is sensitive to small variations in moisture content and dry density of the base and prepared subgrade.

- The CBR value of the base determined from DCP tests generally increase as the seismic modulus increases.

- For granular materials, moduli from laboratory seismic tests are in good agreement with seismic field moduli as long as the laboratory specimens are prepared at the density and moisture content of the field materials. If the specimens are prepared as per Tex-111-E, the laboratory moduli are significantly smaller.

- For granular materials, the laboratory resilient moduli are typically much less than the seismic moduli; this can be attributed to the boundary conditions and the method of sample preparation associated with resilient modulus tests.

- For granular materials, seismic moduli and FWD moduli show similar trends; that is both generally increase; however, they are not related by a unique relationship.

- For AC layer, the seismic moduli measured in situ and seismic moduli measured in the laboratory are quite close.

In the continuation of this project, several issues should be addressed. These issues consists of the following items:

- Develop more comprehensive relationships between the moisture content and dry unit weight and modulus of granular materials.

- Develop relationships between the volumetric properties of ACP and the modulus through monitoring the moduli of specimens prepared for mix design.

- Optimize the source-receiver configuration as a function of the thickness of layers for the PSPA.

- Optimize the source for the granular materials so that enough energy can be coupled into the medium.

- Optimize the coupling of the seismic DCP to the base and subgrade.

- Develop a simplified algorithm for real-time reduction of the DCP data.

- Optimize the source-receiver configuration for the combined seismic/deflection device

- Develop an adequate calibration process for the combined seismic/deflection device

7. References

1. Baker M.R., Crain, K., and Nazarian S. (1995), "Determination of Pavement Thickness with a New Ultrasonic Device," Research Report 1966-1, Center for Geotechnical and Highway Materials Research, The University of Texas at El Paso, El Paso, TX, 53 p.

2. Barksdale R.D., Alba J., Khosla P.N., Kim R., Lambe P.C. and Rahman M.S. (1994), "Laboratory Determination of Resilient Modulus for Flexible Pavement Design," Interim Report Project 1-28, Federal Highway Administration, Washington, DC.

3. Boddapati, K.M. and Nazarian S. (1994), "Effects of Pavement-Falling Weight Deflectometer Interaction on Measured Pavement Response," ASTM STP 1198, American Society of Testing and Materials, Philadelphia, PA, pp. 326-340.

4. Finn F., Saraf S., Kulkarini R., Nair K., Smith W., and Abdullah A. (1977), "The Use of Distress Prediction Subsystems for the Design of Pavement Structures," Proceedings, 4th International Conference on the Structural design of Asphalt Pavements, pp. 3-37.

5. Linveh M., Linveh N.A. and Elhadad E. (1997), "Determining a Pavement Resilient Modulus from Portable FWD Testing," Presented at 76th Transportation Research Board Meeting, Washington, DC.

6. Nazarian, S., Baker M.R. and Crain K. (1993), "Development and Testing of a Seismic Pavement Analyzer," Research Report SHRP-H-375, Strategic Highway Research Program, National Research Council, Washington, D.C.

7. Nazarian S., Yuan D., and Baker M. (1995), "Rapid Determination of Pavement Moduli with Spectral-Analysis-of-Surface-Waves Method," Research Report 1243-1, The University of Texas at El Paso, 76 p.

8. Nazarian S., Pezo R., Picornell P. (1996), "An Approach to Relate Laboratory and Field Moduli of Base Materials," Research Report 1336-2F, The University of Texas at El Paso, 159 p.

9. Nazarian S., Baker M., and Crain K. (1997), "Assessing Quality of Concrete with Wave Propagation Techniques," Materials Journal, American Concrete Institute (Accepted for Publication).

10. National Science Foundation (1994), Workshop on Geophysical Techniques for Site and Material Characterization, Atlanta, GA.

11. Rix G. (1996), personal communication

12. Shinn J.D., Timian D.A., Smith E.B., Morlock C.R., Timian S.M., and McIntash, D.E. (1988), "Geotechnical Investigation of the Ground-Based Free Electron Laser Facility, "Report ARA-NED-88-10, Applied Research Associates, South Royalton, VT.

13. Shook J.F., Finn F.N., Witczak M.W., and Monismith C.L. (1982, "Thickness Design of Asphalt Pavements - The Asphalt Institute Method," Proceedings, 5th International Conference on the Structural design of Asphalt Pavements.

Appendix A

Wave Propagation Theory

This appendix introduces the principle of wave propagation and clarifies the relationships between wave velocities and moduli.

For engineering purposes, profiles of most pavement sections can be reasonably approximated by a layered half-space. With this approximation, the profiles are assumed to be homogeneous and to extend to infinity in two horizontal directions. They are assumed to be heterogenous in the vertical direction, often modeled by a number of layers with constant properties within each layer. In addition, it is assumed that the material in each layer is elastic and isotropic.

Seismic Body Waves

Wave motion created by a disturbance within an ideal whole-space can be described by two kinds of waves: compression waves and shear waves. Collectively, these waves are called body waves, as they travel within the body of the medium. Compression and shear waves can be distinguished by the direction of particle motion relative to the direction of wave propagation.

Compression waves (also called dilatational waves, primary waves, or P-waves) exhibit a push-pull motion. As a result, wave propagation and particle motion are in the same direction. Compression waves travel faster than the other types of waves, and therefore appear first in a direct travel-time record.

Shear waves (also called distortional waves, secondary waves, or S-waves) generate a shearing motion, causing particle motion to occur perpendicular to the direction of wave propagation. Shear waves can be polarized. If the directions of propagation and particle motion are contained in a vertical plane, the wave is "vertically polarized." This wave is called an SV-wave. However, if the direction of particle motion is perpendicular to a vertical plane containing the direction of propagation, the wave is "horizontally polarized." This wave is termed an SH-wave. Shear waves travel more slowly than P-waves and thus appear as the second major wave type in a direct travel-time record.

Seismic Surface Waves

In a half-space, other types of waves occur in addition to body waves. These waves are called surface waves. Many different types of surface waves have been identified and described. The two major types are Rayleigh waves and Love waves.

Surface waves propagate near the surface of a half-space. Rayleigh waves (R-waves) propagate at a speed of approximately 90 percent of S-waves. Particle motion associated with R-waves is composed of both vertical and horizontal components, that when combined, form a retrograde ellipse close to the surface. However, with increasing depth, R-wave particle motion changes to a pure vertical and, finally, to a prograde ellipse. The amplitude of motion attenuates quite rapidly with depth. At a depth equal to about 1.5 times the wavelength, the vertical component of the amplitude is about 10 percent of that at the ground surface.

Particle motion associated with Love waves is confined to a horizontal plane and is perpendicular to the direction of wave propagation. This type of surface wave can exist only when low-velocity layers are underlain by higher velocity layers, because the waves are generated by total multiple reflections between the top and bottom surfaces of the low-velocity layer. As such, Love waves are not generated in pavement sections.

The propagation of body waves (shear and compression waves) and surface waves (Rayleigh waves) are away from a vertically vibrating circular source at the surface of a homogeneous, isotropic, elastic half-space. Miller and Pursey (1955) found that approximately 67 percent of the input energy propagates in the form of R-waves. Shear and compression waves carry 26 and 7 percent of the energy, respectively. Compression and shear waves propagate radically outward from the source. R-waves propagate along a cylindrical wave front near the surface. Although, body waves travel faster than surface waves, body waves attenuate in proportion to $1/r^2$, where r is the distance from the source. Surface wave amplitude decreases in proportion to $1/r^{0.5}$.

Seismic Wave Velocities

Seismic wave velocity is defined as the speed at which a wave advances in the medium. Wave velocity is a direct indication of the stiffness of a material; higher wave velocities are associated with higher stiffness. By employing elastic theory, compression wave velocity can be defined as

$$V_p = [(\lambda + 2G)/\rho]^{0.5} \tag{A.1}$$

where

V_p	=	compression wave velocity,
λ	=	Lame's constant,
G	=	shear modulus, and
ρ	=	mass density.

Shear wave velocity, V_s, is equal to

$$V_s = (G/\rho)^{0.5} \tag{A.2}$$

Compression and shear wave velocities are theoretically interrelated by Poisson's ratio

$$V_p/V_s = [(1 - v)/(0.5 - v)]^{0.5} \tag{A.3}$$

where v is the Poisson's ratio. For a constant shear wave velocity, compression wave velocity increases with an increase in Poisson's ratio. For a v of 0.0, the ratio of V_p to V_s is equal to $\sqrt{2}$; for a v of 0.5 (an incompressible material), this ratio goes to infinity.

For a layer with constant properties, R-wave velocity and shear wave velocity are also related by Poisson's ratio. Although, the ratio of R-wave to S-wave velocities increases as Poisson's ratio increases, the change in this ratio is not significant. For Poisson's ratio of 0.0 and 0.5, this ratio changes from approximately 0.86 to 0.95, respectively. Therefore, it can be assumed that the ratio is equal to 0.90 without introducing an error larger than about 5 percent.

Equation A.3 can be rewritten as

$$v = [0.5(V_p/V_s)^2 - 1]/[(V_p/V_s)^2 - 1] \tag{A.4}$$

This equation can then be used to calculate Poisson's ratio once V_s and V_p are known.

Elastic Constants

Propagation velocities per se have limited use in engineering applications. In pavement engineering, Young's moduli of the different layers should be measured. Therefore, calculating the elastic moduli from propagation velocities is important.

Shear wave velocity, V_s, is used to calculate the shear modulus, G, by

$$G = \rho V_s^2 \tag{A.5}$$

in which ρ is the mass density. Mass density is equal to Υ_t/g, where Υ_t is the total unit weight of the material, and g is gravitational acceleration. If Poisson's ratio (or compression wave velocity) is known, other moduli can be calculated for a given V_s. Young's and shear moduli are related by

$$E = 2G(1 + v) \tag{A.6}$$

or

$$E = 2\rho V_s^2(1 + v) \tag{A.7}$$

In a medium where the material is restricted from deformation in two lateral directions, the ratio of axial stress to axial strain is called constrained modulus. Constrained modulus, M, is defined as

$$M = \rho V_p^2 \tag{A.8}$$

or in terms of Young's modulus and Poisson's ratio

$$M = [(1 - v)E]/[(1 + v)(1 - 2v)] \tag{A.9}$$

The Bulk modulus, B, is the ratio of hydrostatic stress to volumetric strain and can be determined by

$$B = M - (4/3)G \tag{A.10}$$

Appendix B

Simplified Laboratory Testing

One of the major goals of the project is to develop field tests that are compatible with laboratory results. As indicated before, the existing tests used to determine the modulus of AC, base and subgrade in the laboratory are cumbersome and time-consuming. Simplified laboratory tests can be used in conjunction with the more sophisticated ones during the design process. By combining the results from simplified and more comprehensive tests, one can either ensure compatibility or can develop correlations that can be readily used in the field. We used two of these tests, ultrasonic wave propagation device, and free-free resonant column tests in this study.

There is another significant advantage to these tests. The laboratory and field tests can be directly compared since they are based on the same theory and they are generally performed around the same frequency ranges.

Free-Free Resonant Column for Determining Modulus of Base

A schematic of the test set-up is shown in Figure B-1. The specimen is suspended from two wires. An accelerometer is securely placed on one end of the specimen, and the other end is impacted with a hammer instrumented with a load cell. The signals from the accelerometer and load cell are used to determine the resonant frequency, f. Once the frequency, mass density, ρ, and the length of the specimen, L, are known, Young's modulus can be found from

$$E = \rho \, (2 \, f \, L)^2. \tag{B-1}$$

Alternatively, the accelerometer can be placed in the radial direction, and the specimen can be impacted in the radial direction to determine the shear modulus. Once again, the shear and Young's moduli can be combined to calculate Poisson's ratio.

The modulus estimates from free-free resonant column and field tests at one site are shown in Figure B-2. In general the method is quite repeatable, is nondestructive. In less than 3 minutes, the sensors can be placed, tests can be performed and interpreted. The initial equipment cost is about $4,000.
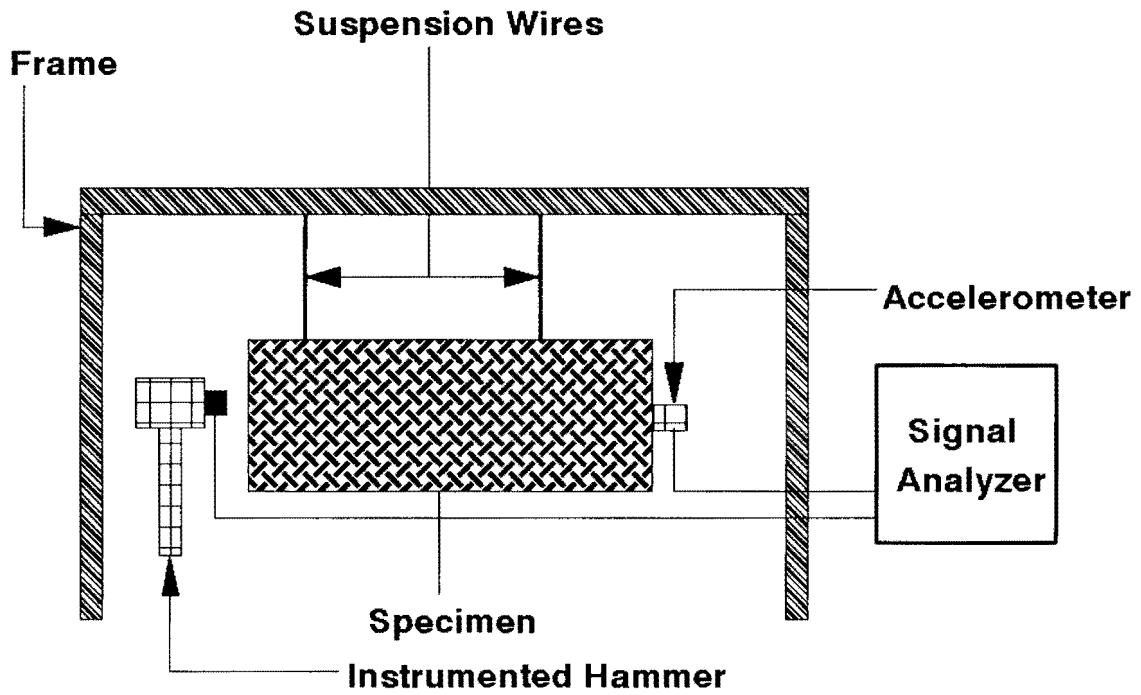
Figure B-1 - Free-Free Resonant Column

Ultrasonic Laboratory Device for Determining Modulus of AC

We have extensively used the device in Project 1369 for testing AC brikettes. The equipment can be purchased from a vendor, and we have developed all the supporting equipment needed to perform the test in day-to-day projects. The device is particularly useful for testing AC brikettes and stabilized layers. The schematic of the testing setup is shown in Figure B-3. A transmitting transducer is securely placed on the top face of the specimen. This transducer is connected to the built-in high-voltage electrical pulse generator of the device. The electric pulse transformed to mechanical vibration was coupled to the specimen. A receiving transducer is securely placed on the bottom face of the specimen, opposite the transmitting transducer. The receiving transducer, which sensed the propagating waves, was connected to an internal clock of the device. The clock has the capability to automatically measure the travel-time of compression waves. A typical measurement would take less than one minute, and the device costs about $ 5,000.
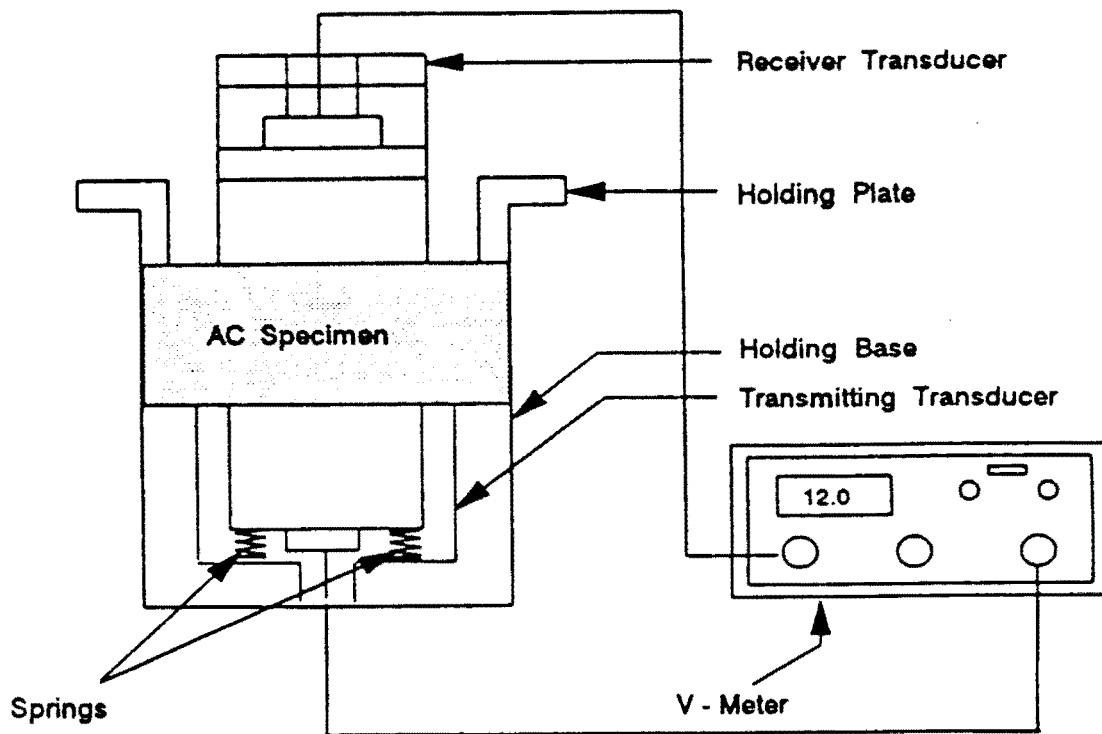
Figure B-2 - Ultrasonic Laboratory Device